3) and IRF-7, promoting their dimerization, nuclear translocation and transcription of IFN-stimulated genes (ISGs), such as ISG56, as well as IFN and other cytokines (Medzhitov, 2007; Platanias, 2005). On the other hand, secreted IFNs bind to the IFN-α/β receptor on the surface of adjacent cells and activate the Janus kinase–signal transducer and activator of transcription (JAK/STAT) signaling pathway, which amplifies IFN induction and stimulates transcription of a variety of antiviral genes (Samuel, 2001). Many viruses encode specific proteins to inhibit IFN induction or the JAK/STAT pathway (Katze et al., 2002; Sen, 2001). The V protein of measles virus (MV) blocks the IFN-inducing pathway mediated by MDA5 and the JAK/STAT pathway (Ohno et al., 2004; Nakatsu et al., 2008). The C protein of MV acts as a regulator of viral RNA synthesis, thereby acting indirectly to suppress IFN induction (Nakatsu et al., 2008).

It has been reported that wild-type measles strains barely induce type I IFN (Naniche et al., 2000; Shingai et al., 2007). The levels of IFN protein or mRNA are lower than the detection limit in cells infected with wild-type MV, while higher levels of IFN are detectable in cells infected with vaccine strains. Although the mechanism behind the strain-to-strain differences in IFN-inducing potential remain unclear, an early report suggested that a laboratory strain, strain Edmonston (ED), possesses a unique V protein with low suppression of IFN-α/β receptor (IFNAR)-amplifiable IFN induction (Ohno et al., 2004). We previously reported that vaccine/laboratory strains harbor defective interference (DI) RNA which activates RIG-I and/or MDA5. Type I IFN is efficiently yielded by DI RNA during viral RNA replication (Shingai et al., 2007). We found that the majority of measles vaccine and laboratory-adapted strains possess DI RNA. However, the IFN-inducibility of attenuated MV strains does not always correlate with the presence of DI RNA. Therefore, the mechanisms by which the primary IFN-inducing activity by RIG-I/MDA5 is impaired during wild-type measles infection still remain unexplained.

In this study, using wild-type and DI-negative attenuated measles strains, we investigated the predominate mechanisms that act on the host IFN system to modulate IFN production. We identified amino acid differences between the V proteins of the attenuated ED strain and wild-type MV, and found that the cysteine residue at position 272 (272C) was required for suppression of MDA5-induced type I IFN production.

2. Materials and methods

2.1. Cell culture and reagents

The human lung epithelial cell line (A549), A549/CD150, African green monkey kidney cell line (Vero), Vero/CD150 and HEK293FT cells were maintained in DMEM supplemented with 10% heat-inactivated FCS and antibiotics (Tanabe et al., 2003). HeLa cells were cultured in Eagle's MEM with 10% heat-inactivated FCS and L-glutamine. For establishing CD150-expressing A549 and Vero cell lines, pCNX2-huCD150 was introduced into cell lines using FugeneHD (Roche) according to the manufacturer's protocol. Twenty-four hours after transfection, the neomycin analog G418 (Sigma–Aldrich) was added to the medium at the final concentration of 1.4 mg/ml or 0.6 mg/ml for Vero or A549 cells. During selection, G418-containing medium was changed once every 4 days. G418-resistant, stably transfected clones were propagated for the study of surface expression of CD150 by flow cytometer. The following antibodies were obtained commercially: anti-FLAG (Sigma–Aldrich); anti-Myc (Santa Cruz); anti-IRF-3 (IBL). Alexa Fluor 488- and Alexa Fluor 568-conjugtaed secondary antibodies were from Invitrogen Life Technologies. Polyriboinosinic/polyribocytidylic acid (polyI:C) was from Amersham Biosciences.

2.2. Plasmids

Complementary DNAs of human TICAM-1, MDA5, RIG-I, V and C were cloned in our laboratory by RT-PCR and ligated into the cloning site of the expression vector, pEF-BOS, pcDNA4 Myc-HisA and pCMV10-FLAG (Funami et al., 2008). Mutations were introduced by site-directed mutagenesis using PCR. All constructs were confirmed by sequencing.

2.3. Virus preparation and titration

Nagataha (NV) and Edmonston (ED) strains were obtained from Dr. S. Ueda (the Research Institute for Microbial Diseases, Osaka University, Osaka, Japan) and University of Washington (Seattle, WA), respectively. Ichinose (IC)-B was provided from Dr. F. Kobune (National Institutes of Health, Tokyo, Japan) (Kubune et al., 1990). Masusako (MS) was propagated in our laboratory (Kurita-Taniguchi et al., 2000; Murabayashi et al., 2002). NV, ED and MS strains were maintained in Vero/CD150 cells in our laboratory (Shingai et al., 2007). IC-B strain was maintained in B95a cells. Virus titer was determined as PFUs on Vero/CD150 and the multiplicity of the infection (MOI) of each experiment was calculated based on this titer (Kubune et al., 1990).

2.4. RT-PCR and real-time PCR

Total RNA was prepared using TRIzol Reagent (Invitrogen) following the manufacturer's instructions. RT-PCR was carried out using the High Capacity cDNA Reverse Transcription kit (Applied Biosystems) according to the manufacturer's instructions. The following oligonucleotides were used for human GAPDH: 5′-TCCACCACCCTGTTGCTGTA-3′ and 5′-ACCACAGTCCATGCCATCAC-3′; and for MV-H: 5′-CCCTTATCAACGGATGATCC-3′ and 5′-GTGATCAATGGCCCCAATCC-3′; and for q-PCR human β-actin: 5′-CCTGGCACCCAGCACAAT-3′ and 5′-GCCGATCCACACGGAGTACT-3′; and for *q*-PCR human IFN-β: 5′-CAATTGCTTGGATTCCTACAAAG-3′ and 5′-TATTCAAGCCTCCCATTCAATTG-3′. IFN-β mRNA were normalized to β-actin and fold inductions of transcripts were calculated using the ddCT method relative to unstimulated HeLa cells.

2.5. RT-PCR amplification of cDNA from 5′ copy-back DI RNAs

We modified the RT-PCR amplification protocol of Calain et al. (1992), where the copy-back DI RNAs were amplified using two set of MV primers (for 5′ copy-back DIs, JM396; 5′-TATAAGCTTACCAGACAAAGCTGGGAATAGAAACTTCG-3′/JM403; 5′-CGAAGATATTCTGGTGTAAGTCTAGTA-3′, and for standard genome, JM396/JM402; 5′-TTTATCCAGAATCTCAARTCCGG-3′) (Sidhu et al., 1994; Whistler et al., 1996). Viral RNA from the culture supernatant was extracted with QIAamp Viral RNA Mini kit (Qiagen). Total RNA from viral-infected cells was extracted with TRIzol Reagent following the manufacturer's instructions. RT-PCR was carried out using the High Capacity cDNA Reverse Transcription kit (Applied Biosystems) according to the manufacturer's instructions. The PCR-amplified products were confirmed by sequencing.

2.6. Reporter gene assay

Cells were seeded onto 24-well plates and transfected with various amounts of expression vectors, the reporter gene, and the phRL-TK control plasmid using FuGene HD (Roche) according to the manufacturer's instructions. After 24 h, the cells were harvested in 100 μl lysis buffer. The luciferase activity was measured using Dual-

Luciferase Reporter assay systems (Promega) and was shown as the means ± S.D. of three experiments.

2.7. Native PAGE, SDS-PAGE, Western blotting, and immunoprecipitation assay

Cells were solubilized in the lysis buffer (50 mM Tris–HCl pH 7.4, 150 mM NaCl, 1.5 mM $MgCl_2$, 1% NP-40, protease inhibitor cocktail, 0.1 mM PMSF, 50 mM NaF, and 1 mM Na_3VO_4) on ice for 30 min and then centrifuged at 12,000 × *g* for 10 min at 4 °C. The supernatants were separated by SDS-PAGE, and the gel was transferred onto polyvinylidene difluoride membranes. The membranes were then blocked with Tris-buffered saline (TBS) pH 8.0 containing 5% skim milk, immunoblotted with specific antibodies, and visualized with the appropriate horseradish peroxidase-conjugated secondary antibodies using the ELC plus Western Blotting Detection System (Amersham Pharmacia). For detection of IRF3-dimerization, whole cell extracts were subjected to 7.5% polyacrylamide gel Native (Daiichi Pure Chemicals). For immunoprecipitation, cells were lysed in the Triton X-100 lysis buffer (50 mM Tris–HCl pH 7.4, 150 mM NaCl, 1.5 mM $MgCl_2$, 1% Triton X-100, 10% glycerol, protease inhibitor cocktail, 0.1 mM PMSF, 50 mM NaF, and 1 mM Na_3VO_4) and then centrifuged at 12,000 × *g* for 10 min at 4 °C. The supernatants were incubated with anti-Myc antibody and protein G-Sepharose (Amersham Pharmacia) for overnight at 4 °C. The immunoprecipitates were collected by centrifugation, washed 4 times in the lysis buffer, and then analyzed by SDS-PAGE.

2.8. Confocal microscopy

HeLa cells (2.5×10^4 cells/well) were plated on a micro cover glass (Matsunami Glass) in 12-well plate. The following day, cells were transfected with the indicated plasmids using FuGENE HD (Roche). The total amounts of DNA were kept constant by adding empty vector. After 24 h, cells were fixed in acetone and blocked in PBS containing 1% BSA and then labeled with the indicated primary antibodies for 1 h at room temperature. Alexa Fluor 488- or Alexa Fluor 594-conjugtaed secondary antibodies were used for the visualizing proteins detected by the primary antibodies. For nucleus staining, cells were treated with DAPI in PBS. After all staining procedures were finished, micro cover glasses were mounted onto a slide glass using PBS containing 2.3% DABCO and 50% glycerol. Cells were visualized at 63× magnification under an LSM510 META microscope (Zeiss).

2.9. Statistical analysis

The statistical significance was analyzed using Student's *t*-test. *p* values < 0.05 were considered significant.

3. Results

3.1. Laboratory adapted strain ED induces IFN-β mRNA in A549/CD150 cells

We tested whether MV induced the expression of IFN-β mRNA in infected A549/CD150 cells and found that laboratory-adapted strain ED induced IFN-β mRNA expression, whereas IFN-β mRNA was virtually undetectable in wild-type strain MS-infected cells (Fig. 1A). To confirm the efficiency of virus infection, we measured MV-H mRNA levels by RT-PCR (Fig. 1B). The MV-H mRNA level in MS-infected cells was comparable to that found in ED-infected cells. Our previous report showed that DI RNA in MV isolates is a crucial determinant for high IFN induction (Shingai et al., 2007). However, no amplifiable 5′ copy-back DI RNA was detected in the MV culture supernatants (Fig. 1C), suggesting that the ED and MS strains used

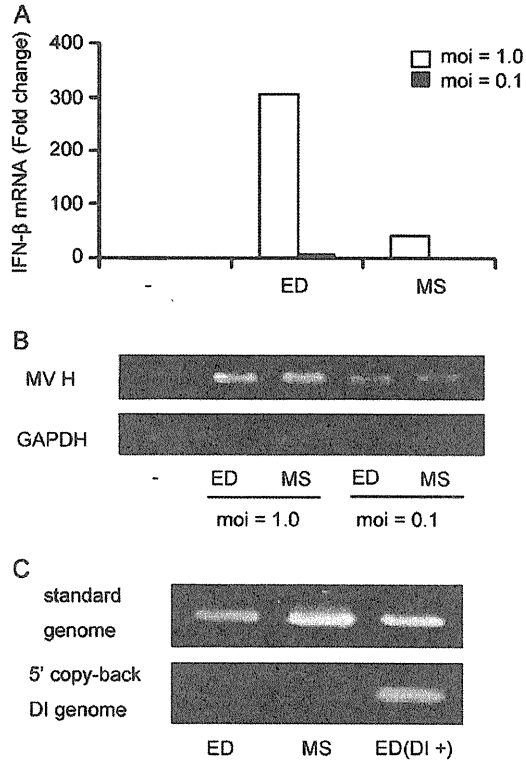

Fig. 1. ED strain induces IFN-β mRNA expression in the infected cells. (A) A549/CD150 cells were infected with mock, ED (vaccine strain) or MS (wild-type strain) at MOI = 0.1 or 1. After 12 h, RNA samples were collected and mRNAs of IFN-β and β-actin were measured by real-time PCR. The value for IFN-β mRNA expression was normalized to that of β-actin mRNA. Fold induction against control medium is shown. (B) MV-H mRNA level was determined by RT-PCR. (C) RT-PCR amplification of 5′ copy-back DI RNA from MV culture supernatants. RT-PCR was performed using standard genome-specific primers or DI-specific primers.

in this study, do not contain 5′ copy-back DI RNA. Thus, in this DI RNA-negative ED strain, a factor other than DI RNA is implicated in the induction of IFN-β mRNA.

3.2. The ED-V protein barely suppresses MDA5-induced IFN-β promoter activity

To explain the differential type I IFN-inducing abilities of ED versus wild-type strains, we transfected cDNAs encoding MV proteins into A549/CD150 cells, established in our laboratory (Tanabe et al., 2003). In these pilot studies, we found that expression of MV V protein suppresses IFN-β promoter activation, as reported by other groups (Nakatsu et al., 2008; Ohno et al., 2004; Takeuchi et al., 2003). We then focused on the function of the V and C proteins of various MV strains. The V and C proteins of MV are not essential products (Radecke and Billeter, 1996) but play important roles in MV virulence (Patterson et al., 2000). The V protein has been shown to inhibit IFN induction via binding to MDA5 (Childs et al., 2007, 2009). On the other hand, the C protein does not block the IFN-inducing pathway, but affects infectivity by acting as a regulator of viral RNA synthesis (Nakatsu et al., 2008). When A549/CD150 cells were stimulated with polyI:C or transfected with RIG-I or MDA5, efficient IFN-β promoter activation was detected using a reporter assay (Fig. 2A–C). Using this assay, we examined the effects of the transfected V and/or C proteins on IFN-β promoter activity. PolyI:C-induced IFN-β promoter activation was inhibited by the V protein expressed by wild-type strains, MS and IC-B, and an attenuated NV strain, which possesses DI RNA (Shingai et al., 2007). The ED-V pro-

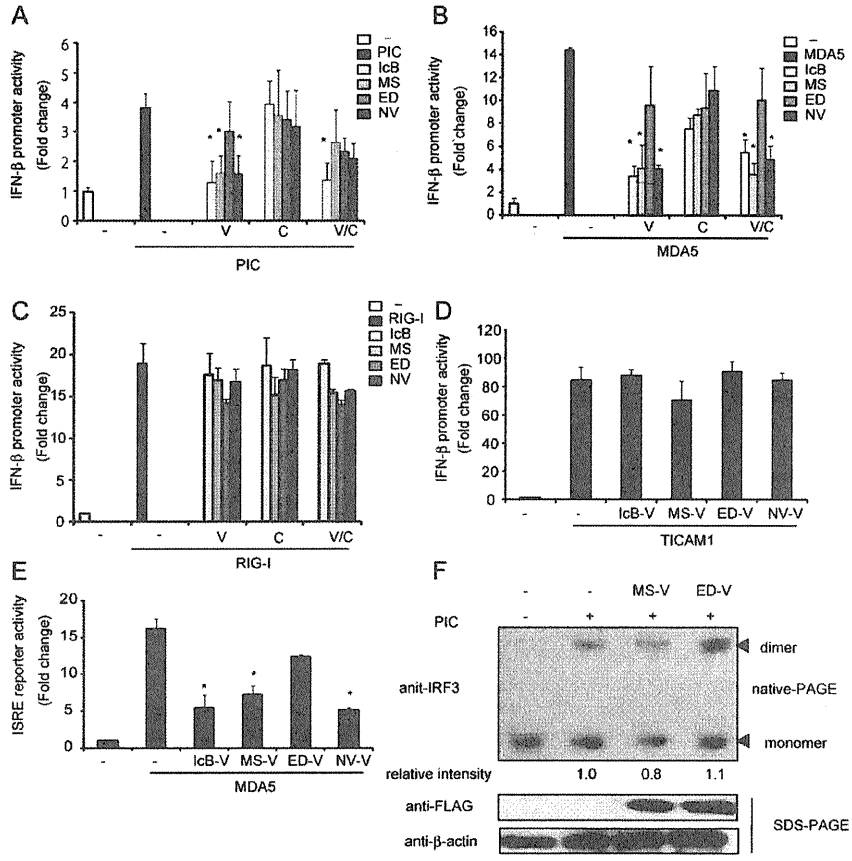

Fig. 2. Strain-to-strain difference in V protein function for MDA5-induced IFN-β promoter activation. (A) A549 cells in 24-well plates were transfected with pCMV10-MV-V (100 ng) and pCMV10-MV-C (100 ng) together with the IFN-β promoter reporter (100 ng) and phRL-TK (50 ng). Twenty-four hours after transfection, the cells were stimulated with 50 μg/ml polyI:C for 6 h, and then the luciferase reporter activity was measured. The average activities from three independent assays are shown as fold induction. A549 cells in 24-well plates were transfected with pEF-BOS FLAG-MDA5 (100 ng, B), pEF-BOS RIG-I (100 ng, C), pEF-BOS TICAM1 (100 ng, D), pCMV10-MV-V (100 ng) and pCMV10-MV-C (100 ng) together with the IFN-β promoter reporter (100 ng) and phRL-TK (50 ng). Twenty-four hours after transfection, the luciferase reporter activity was measured. (E) A549 cells in 24-well plates were transfected with pCMV10-MV-V (100 ng) and pCMV10-MV-C (100 ng) together with the ISRE luciferase gene (100 ng) and phRL-TK (50 ng). Twenty-four hours after transfection, the luciferase reporter activity was measured. The average activities from three independent assays are shown as fold induction. $^*p < 0.05$. (F) HeLa cells transfected with pCMV10 FLAG-MV-V (100 ng). After 24 h, cells were stimulated with 10 μg/ml polyI:C for 1 h and then lysed with native-PAGE lysis buffer or SDS-PAGE lysis buffer. For native-PAGE, the cell lysates were subjected to native-PAGE and immunoblotted with anti-IRF-3 antibody. For SDS-PAGE the cell lysates were subjected to SDS-PAGE and immunoblotted with anti-FLAG antibody or anti-β-actin (internal control). The band intensity was quantified by NIH Image J and relative band intensity was shown. The results were reproducible in three additional experiments.

tein barely suppressed polyI:C-induced IFN-β promoter activation (Fig. 2A). None of the C proteins analyzed affected IFN-β promoter activation.

PolyI:C is regarded as an analog of viral dsRNA and activates TLR3 in the endosomes and RIG-I/MDA5 in the cytoplasm. TLR3 recruits TICAM-1 while RIG-I and MDA5 recruit IPS-1 as adaptors. The two pathways converged upon NAP1, which assembles IKKε and TBK1 to activate IRF-3 and promote induction of IFN-β (Sasai et al., 2006b). Production of a trace amount of IFN-β results in amplified production of type I IFN via the IFNAR pathway, as controlled by the ISRE promoter (Takaoka and Yanai, 2006). To reveal the target pathway inhibited by the V protein of wild-type MV, we examined whether the wild-type MV V proteins block IFN-β induction in cells containing overexpressed MDA5, RIG-I or TICAM-1 (Fig. 2B–D). The V proteins of strains MS and IC-B inhibited MDA5-induced IFN-β and ISRE promoter activation but barely affected RIG-I and TICAM-1-induced IFN-β induction (Fig. 2B–E). It is notable that in our setting, V proteins of various MV strains did not suppress RIG-I-mediated activation of IFN-β promoter (Fig. 2C). These data suggested that the V proteins of wild-type strains suppress the MDA5 pathway for type I IFN induction while the C proteins barely affect MDA5-, RIG-I- and TICAM-1-dependent IFN-β transcription. Under these conditions, only the V protein of strain ED abrogates the inhibitory function of MDA5 in both IFN-β and ISRE reporters.

IRF-3 activation in the cytoplasm occurs via C-terminal phosphorylation of IRF-3 by the TBK1/NAP1/IKKε complex. These modifications promote IRF-3 homodimerization and the subsequent nuclear import of these molecules (Medzhitov, 2007; Platanias, 2005). In our studies for detection of IRF-3 dimer formation, although the V protein of the wild-type strain suppressed polyI:C-induced IRF-3 dimerization, the ED-V protein hardly inhibited polyI:C-induced IRF-3 dimerization (Fig. 2F). These data suggested that the V protein of wild-type strains inhibited polyI:C-induced IFN-β induction via the suppression of MDA5-meditaed IRF-3 activation. To exclude the possibility that the MV-V protein causes MDA5 degradation, we confirmed the MDA5 protein level by Western blotting (Fig. 3). The MDA5 protein levels in the MS-V or ED-V transfected cells were comparable to those found in untreated cells.

3.3. 272C is responsible for suppression of MDA5-induced IFN-β promoter activity

To reveal the molecular mechanism that determines whether MV V protein inhibits MDA5-induced IFN-β promoter activity, we compared the amino acid sequence of the ED V protein with that of

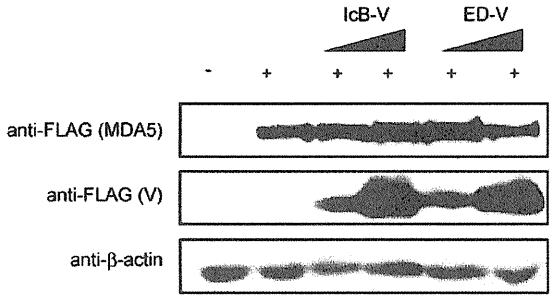

Fig. 3. Forced expression of V protein did not affect the expression level of MDA5 protein. HEK 293FT cells were transfected with pEF-BOS FLAG-MDA5 (100 ng) and pCMV10 FLAG-MV-V (10 ng, 100 ng). After 24 h, cells were lysed and subjected to Western blotting with anti-FLAG antibody and anti-β-actin antibody (internal control).

wild-type V proteins. As shown in Fig. 4, we identified 7 amino acid substitutions (51R, 83P, 97P, 110H, 225G, 272R and 291H) in the ED V protein. These conversions are ED strain V-specific, since the authentic V sequence is conserved in other strains. We then constructed R51K, P83S, P97S, H110Y, G225E, R272C and H291Y mutants of ED V protein and examined the effects of these mutants on MDA5-induced IFN-β promoter activity (Fig. 5A). As shown in Fig. 5A, only R272C mutant of ED V protein suppressed MDA5-activated IFN-β promoter. Next, we examined whether the V protein inhibited polyI:C-induced IRF-3 nuclear translocation. Although WT ED V protein did not inhibit polyI:C-induced IRF-3 nuclear translocation, overexpression of R272C mutant suppressed IRF-3 nuclear translocation (Fig. 5B and C). R51K, P83S, P97S, H110Y, G225E and H291Y mutants did not affect IRF-3 nuclear translocation. Since previous reports have shown that the V proteins of paramyxoviruses interacted with MDA5 to inhibit MDA5 activity and suppress IFN-β induction (Childs et al., 2007, 2009), we examined the interaction between MDA5 and the V proteins by immunoprecipitation. As expected, only R272C mutant interacted with MDA5, whereas WT ED V and the other mutants did not bind MDA5 (Fig. 5D). These data suggest that the arginine at position 272 in ED V protein is responsible for insuppressible activity of MDA5-induced IFN-β promoter activation. The cysteine residue at position 272 of V protein is conserved among paramyxoviruses. To clarify that 272C is important for suppressive activity of WT V protein, we examined effects of IC-B V C272R mutant on MDA5-induced IFN-β promoter activity. As shown in Fig. 6A, although IC-B V protein suppressed IFN-β promoter activity, C272R mutant was not able to inhibit IFN-β promoter activation. Similarly, C272R mutant did not suppressed poly I:C-induced IRF-3 nuclear translocation and interact with MDA5 (Fig. 6B and C). These data infer that the 272C residue of V protein is crucial for interacting with MDA5 and suppressing IRF-3 activation, which reasons that ED V strains fail to interact with MDA5.

4. Discussion

In this study, we demonstrated that the V protein of MV strain ED neither interacted with MDA5 nor suppressed MDA5-induced IRF-3 activation. A C272R mutation in the cysteine-rich region of wild-type V protein rendered the V protein IFN-insuppressible and the R272C conversion in ED strains conferred an IFN-suppressive function on the V protein. The V protein targets MDA5 and V proteins possessing the 272C residue co-precipitate with MDA5 by immunoprecipitation. Only V proteins possessing the 272C residue accelerate nuclear translocation of IRF-3. Based on the results of our reporter assay, V protein does not affect TICAM-1- or RIG-I-induced IFN-β promoter activation. Hence, the 272C residue is crucial for the V protein to block MDA5 function and MDA5 is the molecule which V protein targets for inhibition of the initial induction of IFN-β. For this reason, the ED strain used in this study allowed infected cells to induce IFN-β mRNA even in the absence of DI RNA. A previous report showed that the V protein of Sendai virus binds MDA5 via the cysteine-rich region which is conserved among paramyxoviruses (Childs et al., 2009). Accordingly, we found that the MV V protein interacted with MDA5 via the cysteine-rich region.

```
MS-V     1 MAEEQARHVKNGLECIRALKAEPIGSLAIGEAMAAWSEISDNPGQERATCKEEKAGGSGL 60
IC-B-V   1 MAEEQARHVKNGLECIRALKAEPIGSLAVEEAMAAWSEISDNPGQDRATCKEEEAGSSGL 60
NV-V     1 MAEEQARHVKNGLECIRALKAEPIGSLAIGEAMAAWSEISDNPGQERATCKEEKAGGSGL 60
ED-V     1 MAEEQARHVKNGLECIRALKAEPIGSLAIEEAMAAWSEISDNPGQERATCREEKAGSSGL 60
           ****************************: ***************:****:**:**.***

MS-V    61 SKPCLSAIGSTEGGAPRIRGQGSGESDDDTETLGIPSRNLQASSTGLQCYYVYDHSGEAV 120
IC-B-V  61 SKPCLSAIGSTEGGAPRIRGQGSGESDDDAETLGIPSRNLQASSTGLQCYHVYDHSGEAV 120
NV-V    61 SKSCLSAVGSTEGGAPRIRGQGSGESDDDTETLGIPSRNLQASSTGLQCYYVYDHSGEAV 120
ED-V    61 SKPCLSAIGSTEGGAPRIRGQGPGESDDDAETLGIPPRNLQASSTGLQCHYVYDHSGEAV 120
           **.****:**************.******:******.************::*********

MS-V   121 KGIQDADSIMVQSGLDGDSTLSGGDNESENSDVDIGEPDTEGYAITDRGSAPISMGFRAS 180
IC-B-V 121 KGIQDADSIMVQSGLDGDSTLSGGDDESENSDVDIGEPDTEGYAITDRGSAPISMGFRAS 180
NV-V   121 KGIQDADSIMVQSGLDGDSTLSGGDNESENSDVDIGEPDTEGYAITDRGSAPISMGFRAS 180
ED-V   121 KGIQDADSIMVQSGLDGDSTLSGGDNESENSDVDIGEPDTEGYAITDRGSAPISMGFRAS 180
           *************************:************************************

MS-V   181 DVETAEGGEIHELLRLQSRGNTLPKLGKTLNVPPPPDPGRASASETPIKKGHRREISLIW 240
IC-B-V 181 DVETAEGGEIHELLKLQSRGNNFPKLGKTLNVPPPPNPSRASTSETPIKKGHRREIGLIW 240
NV-V   181 DVETAEGGEIHELLRLQSRGNTFPKLGKTLNVPPPPDPGRASTSETPIKKGHRREISLIW 240
ED-V   181 DVETAEGGEIHELLRLQSRGNNFPKLGKTLNVPPPPDPGRASTSGTPIKKGHRREISLIW 240
           **************:******.:**************:*. **:* ***********.***

MS-V   241 NGDRVFIDRWCNPMCSKVTLGTIRARCTCGECPRVCEQCRTDTGVDTRIWYHNLPEIPE 299
IC-B-V 241 NGDRVFIDRWCNPMCSKVTLGTIRARCTCGECPRVCEQCRTDTGVDTRIWYHNLPEIPE 299
NV-V   241 NGDRVFIDRWCNPMCSKVTLGTIRARCTCGECPRVCEQCRTDTGVDTRIWYHNLPEIPE 299
ED-V   241 NGDRVFIDRWCNPMCSKVTLGTIRARCTCGERPRVCEQCRTDTGVDTRIWHHNLPEIPE 299
           ****************************** ******************:********
```

Fig. 4. Comparison of the ED V protein amino acid sequences with various MV strain. Several point mutations were found in the ED-V protein. Underline shows the conserved-Cys-rich region. Arrow heads show mutations in ED V protein.

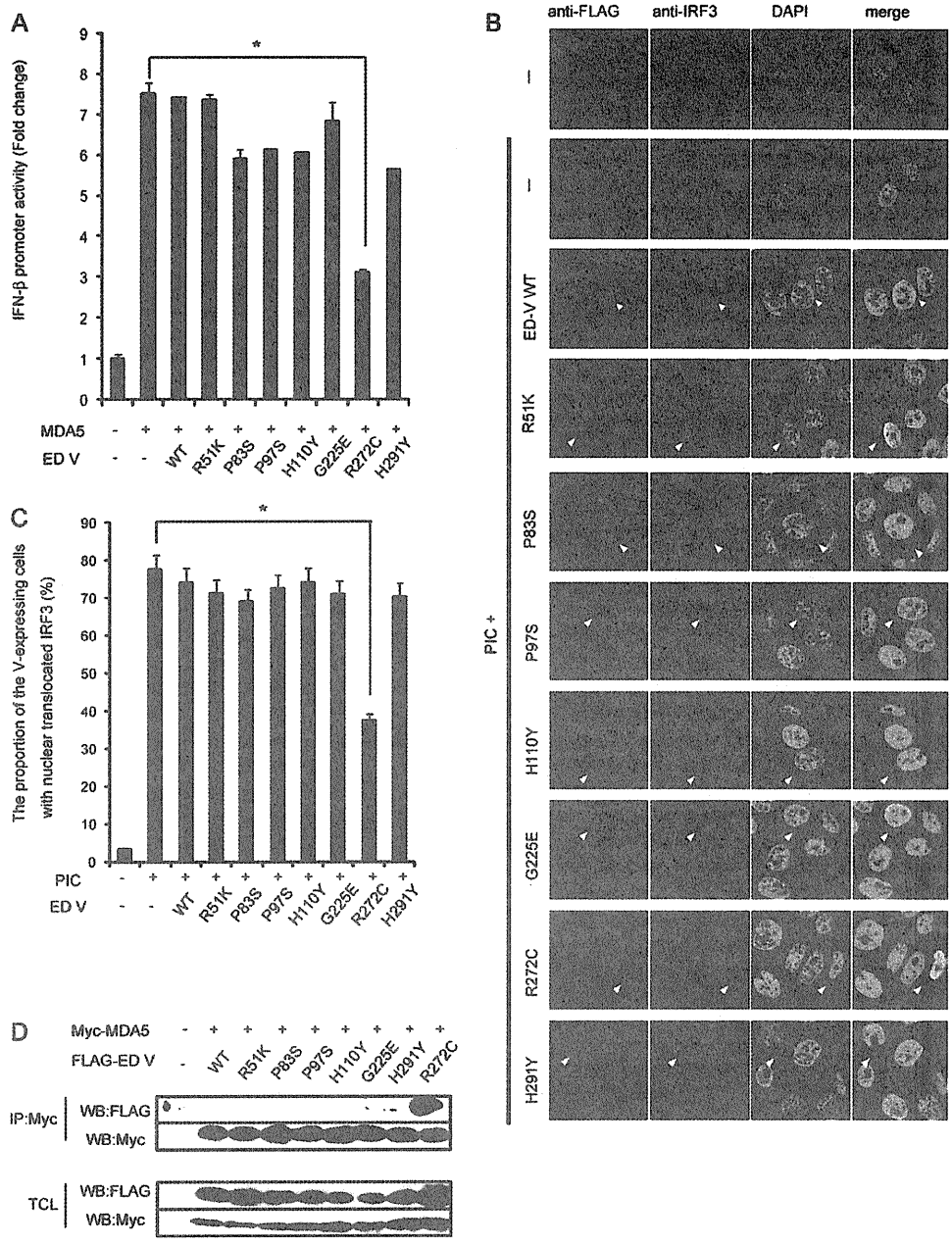

Fig. 5. 272C is a critical residue for suppression of MDA5-induced IFN-β promoter activity. (A) A549 cells in 24-well plates were transfected with pEF-BOS FLAG-MDA5 and pCMV10-MV-V together with the IFN-β promoter reporter and phRL-TK. Twenty-four hours after transfection, the luciferase reporter activity was measured. The average activities from three independent assays are shown as fold induction. *$p < 0.05$. (B) HeLa cells were transfected with various pCMV10 ED-V plasmids. After 24 h, the cells were stimulated with 10 μg/ml polyI:C for 1 h, fixed and stained with anti-IRF-3 and anti-FLAG antibodies (V protein), and visualized with either Alexa Fluor 488- or Alexa Fluor 594-conjugated secondary antibodies. The same slide was also treated with DAPI for the staining of nuclei. Arrow heads show V-expressing cells. (C) The number of the V-expressing cells with nuclear translocated IRF3 (see panel B) were counted. The results are shown by the proportion of the V-expressing cells with nuclear translocated IRF3 ($n = 50$). The average proportions from three independent assays are shown. *$p < 0.05$. (D) HEK293FT cells were transfected with pcDNA4 Myc-MDA5 and pCMV10 FLAG-MV-V with mutations. After 24 h, the cells were lysed, immunoprecipitated with anti-FLAG antibody and immunoblotted with anti-Myc or anti-FLAG antibodies. An aliquot of each total cell lysate (TCL) was immunoblotted with either anti-Myc or anti-FLAG antibodies.

Childs et al. (2009) reported that the V protein of paramyxovirus specifically inhibited activation of the MDA5 pathway, but not the RIG-I pathway, by specifically binding to the helicase domain of MDA5 and hindering MDA5 from recruiting dsRNA. Consistent with their report, the V protein thus blocks sensing dsRNA via MDA5 to disassemble oligomerization of MDA5. These results infer that the IFN-inducible properties of the laboratory-adapted ED strain were largely attributable to the aberrance of the function of the V protein by introduction of the C272R mutation. We only regret that we could not detect the complex of endogenous MDA5 and MV V in this study since resting cells express only a trace amount of MDA5 (Yoneyama et al., 2005).

Ohno et al. (2004) showed that the 110Y and 272C residues of the V protein were responsible for the suppression of IFN-α and IFN receptor signaling using HEK293 transfectants. In contrast, we clarified that C272R mutant but H110Y mutant of ED V protein sup-

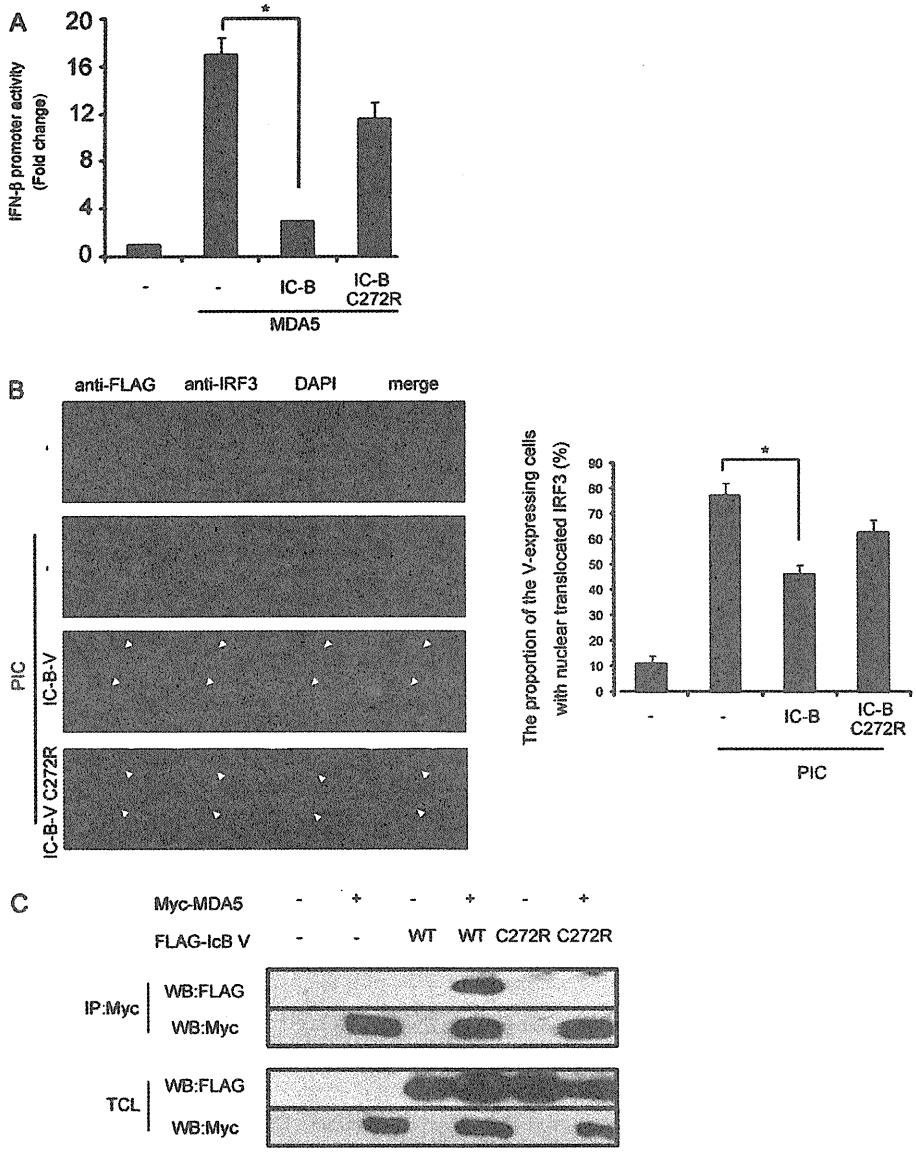

Fig. 6. 272C is important for suppressive activity of WT V protein. (A) A549 cells in 24-well plates were transfected with pEF-BOS FLAG-MDA5 and various pCMV10-IC-B-V plasmids together with the IFN-β promoter reporter and phRL-TK. Twenty-four hours after transfection, the luciferase reporter activity was measured. The average activities from three independent assays are shown as fold induction. *$p < 0.05$. (B) HeLa cells were transfected with various pCMV10 ED-V plasmids. After 24 h, the cells were stimulated with 10 μg/ml polyI:C for 1 h, fixed and stained with anti-IRF-3 and anti-FLAG antibodies (V protein), and visualized with either Alexa Fluor 488- or Alexa Fluor 594-conjugated secondary antibodies. The same slide was also treated with DAPI for the staining of nuclei. Arrow heads show V-expressing cells. Right panel shows the proportion of the V-expressing cells with nuclear translocated IRF3. (C) Immunoprecipitation assay in 293T cells. Cells were transfected with pcDNA4 Myc-MDA5 and pCMV10 FLAG-MV-V. After 24 h, the cells were lysed, immunoprecipitated with anti-FLAG antibody and immunoblotted with anti-Myc or anti-FLAG antibodies. An aliquot of each total cell lysate (TCL) was immunoblotted with either anti-Myc or anti-FLAG antibodies.

pressed IFN-β promoter activity in the MDA5 pathway. Hence, the tyrosine at position 110 is responsible only for blocking the IFN amplification pathway via IFN-α/β receptor (IFNAR). On the other hand, the cysteine residue at position 272 is important for inhibiting both MDA5-induced IFN-β transactivation and IFNAR amplification loop. The V protein of strain ED is unable to block not only MDA5 but also the IFNAR amplification pathway, thereby ED-based vaccine strains would be able to induce type I IFN. Consistent with this possibility, Ikegame et al. (2010) reported the participation of MDA5 in MV-mediated IFN induction and MV growth promotion using RIG-I-silenced cells and V protein-deficient MV strains. In fact, the V proteins of ED and wild-type strains play no role in blocking the downstream of TBK1 for IFN-β reporter activation (data not shown). However, we wonder if the viruses produce sufficient amounts of long dsRNA (>40 bp in length, enough to be detected by J2 mAb) to be recognized by MDA5 in an early step of infection, i.e. before the production of V protein. Since RIG-I recognizes 5′-3P-ssRNA or short dsRNA, the RIG-I pathway is thought to be predominantly involved in IFN induction in MV-infected cells (Plumet et al., 2007; Shingai et al., 2007). Detailed analysis will be required to elucidate the predominant usage of RIG-I or MDA5 for type I IFN induction in cells infected with a variety of viruses. Why MV blocks MDA5 but not RIG-I activity and which viral products specifically recognize and bind MDA5 are questions that remained to be answered.

The C protein of MV plays an important role in inhibiting the JAK-STAT pathway of IFNAR signaling (Shaffer et al., 2003), and also acts

as a regulator of viral RNA synthesis, thereby indirectly suppressing IFN induction (Nakatsu et al., 2006, 2008; Takeuchi et al., 2005). MV mutants that fail to express the C protein allow infected cells to generate dsRNA (Ikegame et al., 2010), suggesting that the C protein may also function in controlling the generation of long dsRNA. In this study, we observed that the forced expression of C protein did not affect polyI:C-, RIG-I- and MDA5-induced IFN-β reporter activity and there were no significant amino acid changes in this protein among wild-type and vaccine strains (data not shown). C protein appears neither to directly affect the IFN-inducing pathways, nor to be responsible for the IFN-induction of vaccine strains. An interesting issue is the relationship between activation of the MDA5 pathway by MV vaccine strains and the limited production of long dsRNA due to the function of the C protein.

In conclusion, our data suggest that the C272R mutation in the V protein in MV strains is a major cause of insuppressible IFN production in a certain case of MV infection and that the 272C residue of the V protein is responsible for the MDA5-blocking ability of wild-type MV. Although RIG-I recognizes MV products including DI RNA or 5′-3P-ssRNA, the initial response of MDA5 also acts as a cause for amplifying type I IFN production, at least in some vaccine strains.

Conflict of interest

There is no conflict of interest in this study.

Acknowledgements

We are grateful to Drs. A. Watanabe, H.H. Aly, H. Shime, J. Kasamatsu, S. Yamazaki, and T. Ebihara for invaluable discussions. This work was supported in part by Grants-in-Aid from the Ministry of Education, Science, and Culture, the Ministry of Health, Labor, and Welfare of Japan, and by the NorthTec Foundation, the Yakult Foundation, Waxman Foundation and the Akiyama Life Science Foundation. Financial support by the Sapporo Biocluster "Bio-S" the Knowledge Cluster Initiative of the MEXT, and the Program of Founding Research Centers for Emerging and Reemerging Infectious Diseases, MEXT are gratefully acknowledged.

References

Bowie, A.G., Fitzgerald, K.A., 2007. RIG-I: tri-ing to discriminate between self and non-self RNA. Trends Immunol. 28, 147–150.
Calain, P., Curran, J., Kolakofsky, D., Roux, L., 1992. Molecular cloning of natural paramyxovirus copy-back defective interfering RNAs and their expression from DNA. Virology 191, 62–71.
Childs, K., Stock, N., Ross, C., Andrejeva, J., Hilton, L., Skinner, M., Randall, R., Goodbourn, S., 2007. mda-5, but not RIG-I, is a common target for paramyxovirus V protein. Virology 359, 190–200.
Childs, K.S., Andrejeva, J., Randall, R.E., Goodbourn, S., 2009. Mechanism of mda-5 inhibition by paramyxovirus V protein. J. Virol. 83, 1465–1473.
Funami, K., Sasai, M., Oshiumi, H., Seya, T., Matsumoto, M., 2008. Homo-oligomerization is essential for Toll/IL-1 receptor domain containing adaptor molecule-1-mediated NF-kappaB and interferon regulatory factor-3 activation. J. Biol. Chem. 283, 18283–18291.
Ikegame, S., Takeda, M., Ohno, S., Nakatsu, Y., Nakanishi, Y., Yanagi, Y., 2010. Both RIG-I and MDA5 RNA helicases contribute to the induction of alpha/beta interferon in measles virus-infected human cells. J. Virol. 84, 372–379.
Katze, M.G., He, Y., Gale Jr., M., 2002. Viruses and interferon: a fight for supremacy. Nat. Rev. Immunol. 2, 675–687.
Kubune, F., Sakata, H., Hayashi, T., 1990. Marmoset lymphoblastoid cells as a sensitive host for isolation of measles virus. J. Virol. 64, 700–705.
Kurita-Taniguchi, M., Fukui, A., Hazeki, K., Hirano, A., Tsuji, S., Matsumoto, M., Watanabe, M., Ueda, S., Seya, T., 2000. Functional modulation of human macrophages through CD46 (measles virus receptor): production of IL-12p40 and nitric oxide in association with recruitment of protein-tyrosine phosphatase SHP-1 to CD46. J. Immunol. 165, 5143–5152.
Medzhitov, R., 2007. Recognition of microorganisms and activation of the immune response. Nature 449, 819–826.
Murabayashi, N., Kurita-Taniguchi, M., Ayata, M., Matsumoto, M., Ogura, H., Seya, T., 2002. Susceptibility of human dendritic cells (DCs) to measles virus (MV) depends on their activation stages in conjunction with the level of CDw150: role of Tol stimulators in DC maturation and MV amplification. Microbes Infect. 4, 785–794.
Nakatsu, Y., Takeda, M., Ohno, S., Koga, R., Yanagi, Y., 2006. Translational inhibition and increased interferon induction in cells infected with C protein-deficient measles virus. J. Virol. 80, 11861–11867.
Nakatsu, Y., Takeda, M., Ohno, S., Shirogane, Y., Iwasaki, M., Yanagi, Y., 2008. Measles virus circumvents the host interferon response by different action of the C and V proteins. J. Virol. 82, 8296–8306.
Naniche, D., Yeh, A., Eto, D., Manchester, M., Friedman, R.M., Oldstone, M.B.A., 2000. Evasion of host defenses by measles virus: wild-type measles virus infection interferes with induction of alpha/beta interferon production. J. Virol. 74, 7478–7484.
Ohno, S., Ono, N., Takeda, M., Takeuchi, K., Yanagi, Y., 2004. Dissection of measles virus V protein in relation to its ability to block alpha/beta interferon signal transduction. J. Gen. Virol. 85, 2991–2999.
Oshiumi, H., Matsumoto, M., Funami, K., Akazawa, T., Seya, T., 2003. TICAM-1, an adaptor molecule that participates in Toll-like receptor 3-mediated interferon-beta induction. Nat. Immunol. 4, 161–167.
Patterson, J.B., Thomas, D., Lewicki, H., Billeter, M.A., Oldstone, M.B., 2000. V and C proteins of measles virus function as virulence factors in vivo. Virology 267, 80–89.
Pichlmair, A., Reis, E., Sousa, C., 2007. Innate recognition of viruses. Immunity 27, 370–383.
Platanias, L.C., 2005. Mechanisms of type-I- and type-II-interferon-mediated signalling. Nat. Rev. Immunol. 5, 375–386.
Plumet, S., Herschke, F., Bourhis, J.M., Valentin, H., Longhi, S., Gerlier, D., 2007. Cytosolic 5′-triphosphate ended viral leader transcript of measles virus as activator of the RIG I-mediated interferon response. PLoS One 14, e279.
Radecke, F., Billeter, M.A., 1996. The nonstructural C protein is not essential for multiplication of Edmonsto B strain measles virus in cultured cells. Virology 217, 418–421.
Samuel, C.E., 2001. Antiviral actions of interferons. Clin. Microbiol. Rev. 14, 778–809.
Sasai, M., Shingai, M., Funami, K., Yoneyama, M., Fujita, T., Matsumoto, M., Seya, T., 2006a. NAK-associated protein 1 participates in both the TLR3 and the cytoplasmic pathways in type I IFN induction. J. Immunol. 177, 8676–8683.
Sasai, M., Matsumoto, M., Seya, T., 2006b. The kinase complex responsible for IRF-3-mediated IFN-{beta} production in myeloid dendritic cells (mDC). J. Biochem. (Tokyo) 139, 171–175.
Sen, G.C., 2001. Viruses and interferons. Annu. Rev. Microbiol. 55, 255–281.
Shaffer, J.A., Bellini, W.J., Rota, P.A., 2003. The C protein of measles virus inhibits the type I interferon response. Virology 315, 389–397.
Shingai, M., Ebihara, T., Begum, N.A., Kato, A., Honnma, T., Matsumoto, K., Saito, H., Ogura, H., Matsumoto, M., Seya, T., 2007. Differential type I IFN-inducing abilities of wild-type versus vaccine strains of measles virus. J. Immunol. 179, 6123–6133.
Sidhu, M.S., Crowley, J., Lowenthal, A., Karcher, D., Menonna, J., Cook, S., Udem, S., Dowling, P., 1994. Defective measles virus in human subacute sclerosing panencephalitis brain. Virology 202, 631–641.
Takaoka, A., Yanai, H., 2006. Interferon signalling network in innate defence. Cell Microbiol. 8, 907–922.
Takeuchi, O., Akira, S., 2008. MDA5/RIG-I and virus recognition. Curr. Opin. Immunol. 20, 17–22.
Takeuchi, K., Kadota, S.I., Takeda, M., Miyajima, N., Nagata, K., 2003. Measles virus V protein blocks interferon (IFN)-alpha/beta but not IFN-gamma signaling by inhibiting STAT1 and STAT2 phosphorylation. FEBS Lett. 545, 177–182.
Takeuchi, K., Takeda, M., Miyajima, N., Ami, Y., Nagata, N., Suzuki, Y., Shahnewaz, J., Kadota, S., Nagata, K., 2005. Stringent requirement for the C protein of wild-type measles virus for growth both in vitro and in macaques. J. Virol. 79, 7838–7844.
Tanabe, M., Kurita-Taniguchi, M., Takeuchi, K., Takeda, M., Ayata, M., Ogura, H., Matsumoto, M., Shingai, M., Ayata, M., Ogura, M., Seya, T., 2003. Mechanism of up-regulation of human Toll-like receptor 3 secondary to infection of measles virus-attenuated strains. Biochem. Biophys. Res. Commun. 311, 39–48.
Whistler, T., Bellini, W.J., Rota, P.A., 1996. Generation of defective interfering particles by two vaccine strains of measles virus. Virology 220, 480–484.
Yoneyama, M., Kikuchi, M., Matsumoto, K., Imaizumi, T., Miyagishi, M., Taira, K., Foy, E., Loo, Y.M., Gale Jr., M., Akira, S., Yonehara, S., Kato, A., Fujita, T., 2005. Shared and unique functions of the DExD/H-box helicases RIG-I, MDA5, and LGP2 in antiviral innate immunity. J. Immunol. 175, 2851–2858.

ELSEVIER

INSTITUT PASTEUR

Microbes and Infection xx (2011) 1–9

www.elsevier.com/locate/micinf

Original article

Failure of mycoplasma lipoprotein MALP-2 to induce NK cell activation through dendritic cell TLR2

Ryoko Sawahata [a,1], Hiroaki Shime [a,1], Sayuri Yamazaki [a], Norimitsu Inoue [b], Takashi Akazawa [b], Yukari Fujimoto [c], Koichi Fukase [c], Misako Matsumoto [a], Tsukasa Seya [a,*]

[a] *Department of Microbiology and Immunology, Graduate School of Medicine, Hokkaido University, N-15 W-7, Kita-ku, Sapporo 060-8638,Japan*
[b] *Department of Molecular Genetics, Osaka Medical Center for Cancer, Nakamichi 1-3-2, Higashinari-ku, Osaka 537-8511, Japan*
[c] *Department of Chemistry, Graduate School of Science, Osaka University, Toyonaka, Osaka 560-0043, Japan*

Received 1 September 2010; accepted 9 December 2010

Abstract

Macrophage-activating lipopeptide 2 (MALP-2), a mycoplasmal diacylated lipopeptide with palmitic acid moiety (Pam2), activates Toll-like receptor (TLR) 2 to induce inflammatory cytokines. TLR2 is known to mature myeloid dendritic cells (mDC) to drive mDC contact-mediated natural killer (NK) cell activation. Here we tested if MALP-2 activates NK cells through stimulation of TLR2 on mDC. Although synthetic MALP-2 with 6 or 14 amino acids (a.a.) stretch (designated as s and f) matured mDC to induce IL-6, IL-12p40 and TNF-α to a similar extent, they far less activated NK cells than Pam2CSK4, a positive control of 6 a.a.-containing diacyl lipopeptide. MALP-2s and f were TLR2/6 agonists and activate the MyD88 pathway similar to Pam2CSK4, but MALP-2s having the CGNNDE sequence acted on mDC TLR2 to barely induce external NK activation. Even the s form, with slightly high induction of IL-6 compared to the f form, barely induced *in vivo* growth retardation of NK-sensitive implant tumor. Pam2CSK4 and MALP-2 have the common lipid moiety but different peptides, which are crucial for NK cell activation. The results infer that MALP-2 is applicable to a cytokine inducer but not to an adjuvant for antitumor NK immunotherapy.

Keywords: Toll-like receptor 2; MyD88; Macrophage-activating lipopeptide 2; Dendritic cells; NK activation

1. Introduction

Macrophage-activating lipopeptide 2 (MALP-2) is a mycoplasmal diacylated lipopeptide with agonistic activity for Toll-like receptor (TLR) 2 [1]. Myeloid dendritic cells (mDC) and macrophages produce inflammatory cytokines in response to MALP-2 [1,2]. MALP-2 is proteolytically liberated from the parent lipoprotein of M161Ag [2,3] or MALP-404 [4], which is anchored on the outer membrane of *Mycoplasma fermentans*. Although the protease that specifically cleaves M161Ag into MALP-2 has not been identified, the peptide sequence of MALP-2 is determined by Mass spectrometry as S-[2,3-bis (palmitoyl)propyl]cysteine (Pam2Cys) followed by 14 amino acids [5] (Table 1). In fact, the TLR2 agonistic functions are conserved in a synthetic compound (herein referred to MALP-2f) [5]. This synthetic MALP-2 has been applied to clinical phase studies to develop a new adjuvant [6].

Several reports suggested that microbial pattern molecules have the ability to activate natural killer (NK) cells *in vitro* [7–10]. TLR and cytoplasmic pattern sensors are representative pattern-recognition receptors (PRR) which may be associated with mDC-mediated NK activation [7–9]. TLR3 and the adapter TICAM-1 (TRIF) in mDC typically participate in driving NK activation in response to dsRNA [10]. Recent studies on TLR2 agonists including lipopeptides also revealed that stimulation of TLR2 on mDC results in activation of the MyD88 pathway in mDC to drive external NK activation [11,12]. NK cells play a role in early defense against various pathogens.

* Corresponding author. Tel.: +81 11 706 5073; fax: +81 11 706 7866.
E-mail address: seya-tu@pop.med.hokudai.ac.jp (T. Seya).
[1] First two authors equally contributed to this work.

1286-4579/$ - see front matter © 2010 Institut Pasteur. Published by Elsevier Masson SAS. All rights reserved.
doi:10.1016/j.micinf.2010.12.003

Table 1
Lipopeptides used in this study.

Name	Peptide structure	Mr (Dalton)	Ref.
Pam2CSK	CSK	887.3	[19]
Pam2CSK4	CSKKKK	1271.8	[13]
Pam2Cys12	CSTSEVIGEKI	1716.2	[19]
MALP-2s	CGNNDE	1201.5	(*)[a]
MALP-2f	CGNNDESNISFKEK	2135.6	[13]

[a] * — This paper.

We have looked into the immuno-modulatory function of M161Ag and MALP-2, to develop a new adjuvant for cancer immunotherapy [1]. MALP-2 possessed high activity to induce IL-6, TNF-α, IL-10 and IL-12p40 from myeloid cells, but its functional potential for NK activation has not been examined yet. We test in the present studies whether MALP-2 has sufficient activity to induce NK cell activation *in vitro* and NK-mediated tumor regression *in vivo* using a mouse tumor implant model.

2. Materials and methods

2.1. Reagents and antibodies

The following materials were obtained as indicated: Fetal calf serum (FCS) from Bio Whittaker (Walkersville, MD), mouse granulocyte-macrophage colony-stimulating factor (GM-CSF) from PeproTech EC, Ltd (London, UK), the enzyme-linked immunosorbent assay (ELISA) kits for mouse (m)IFN-γ from Biolegend (San Diego, CA), IL-12p40, IL-12p70, and IL-6 from eBioscience (San Diego, CA). Two forms of synthetic macrophage-activating lipopeptide 2 (MALP-2) were ordered to Biologica Co., Nagoya, Japan. MALP-2s: Pam2CGNNDE (MW; 1201.5) and MALP-2f: Pam2CGNNDESNISFKEK (MW; 2135.6). The synthesis of lipopeptides was achieved with a combination of solution- and solid-phase methods as described [13]. Pam2Cys12 (Pam_2CSTSEVIGEKI), Pam2CSK4 (Pam_2CSKKKK) and control Pam2CSK were prepared as referenced [12]. PolyI:C, a TLR3 agonist for induction of anti-tumor immunity, was used for this study as a positive control.

The following antibodies were used: fluorescein isothiocyanate (FITC)-labeled anti-mouse CD69, I-Ab, IFN-α mAb, phycoerythrin (PE)-labeled anti-mouse CD86, CD25, and allophycocyanin (APC)-labeled anti-mouse NK1.1 were purchased from Biolegend (San Diego, CA).

2.2. Mouse and cell lines

TLR2−/− and MyD88−/− mice were gifts from Dr. S. Akira (Osaka Univ., Osaka) as previously reported [14]. Female C57BL/6 mice were purchased from Clea Japan (Tokyo). Mice were maintained in our institute under specific pathogen-free conditions. All animal work was performed under guidelines established by the Hokkaido University Animal Care and Use Committee. Mice (12 weeks female C57BL/6) were housed four per cage and allowed food and water ad libitum. Animal studies were carefully performed without ethical problems.

HEK293 cells were obtained from ATCC and maintained in RPMI 1640/10% FCS. B16D8 cells were established in our laboratory as a subline of the B16 melanoma cell line [15] and cultured in RPMI 1640/10% FCS. This subline was characterized by its low MHC levels with no metastatic properties when injected s.c. into syngeneic C57BL/6 mice. The B16D8 cell line is a typical NK target [10].

2.3. Preparation of BMDC and spleen NK cells of mice

Mouse bone marrow-derived DC (BMDC) were prepared as described previously [16]. Spleen NK cells were positively isolated from spleens with DX5 Micro Beads kit (Miltenyi Biotech) [10]. The purity of NK cells ($DX5^+$ cells) was routinely about 80%. $DX5^+$ NK cells were used within 24 h.

2.4. Reporter assay

Plasmids (pEFBos) for expression of human TLR1, TLR2, TLR6 and TLR10 were prepared in our laboratory as described previously [16]. HEK293 cells were seeded onto 24-well plates and transfected with various amounts of expression vectors, the ELAM reporter gene, and the phRL-TK control plasmid using FuGene HD (Roche) according to the manufacturer's instructions. After 24 h, the cells were harvested in 50 μl lysis buffer. The luciferase activity was measured using Dual-Luciferase Reporter assay systems (Promega) and was shown as the mean ± S.D. of three experiments.

2.5. ELISA, flow cytometric (FACS) analysis of cell surface antigens

The levels of cytokines (IL-6, IL-12p40, IFN-γ etc.) were determined by sandwich ELISA (Amersham Pharmacia Biotech, Buckinghamshire, UK) or the message levels assessed by quantitative PCR [27]. Surface CD86 and I-Ab were determined by FACS using specific mAbs. The practical methods for FACS were described previously [16].

2.6. Assessment of in vitro cytolytic activity

The cytolytic activity of spleen NK cells was determined by ^{51}Cr assay as described previously [10]. NK cells were prepared from the spleen of C57BL/6 mice. NK cells were co-cultured with BMDCs at a ratio of 2:1 and 24 h later the mixtures were subdivided to assess NK-mediated cytotoxicity [10]. A B16 subline (D8) was used as a target cell. Target cells (2×10^3 cells/well) were coincubated with NK cells at the indicated lymphocyte to target (E/T) cell ratio (typically 20) in U-bottom 96-well plates in a total volume of 200 μl of RPMI 1640/10% FCS medium at 37 °C. Four hours later, the liberated ^{51}Cr in the medium was measured using the scintillation counter. Specific cytolytic activity was obtained by the formula: Specific cytotoxic activity (%) = [(experimental ^{51}Cr activity − spontaneous ^{51}Cr activity)/(total ^{51}Cr activity − spontaneous ^{51}Cr activity)] × 100. Each experiment was done in triplicate to confirm reproducibility of the results, and representative results are shown.

Please cite this article in press as: R. Sawahata, et al., Failure of mycoplasma lipoprotein MALP-2 to induce NK cell activation through dendritic cell TLR2, Microbes and Infection (2011), doi:10.1016/j.micinf.2010.12.003

2.7. Tumor challenge and the treatment with Pam2Cys-containing peptides

B16D8 cells (6×10^5 cells) were subcutaneously (s.c.) transplanted into the back of mice at day 0. Pam2Cys-containing peptides (10 μg/head) or PBS (vehicle) only were injected around tumor at day 0, 3, 7, 9, 13, and 17. Tumor surfaces were measured twice a week by using a caliper.

3. Results

3.1. BMDC maturation and cytokine liberation in response to MALP-2

Pam2Cys-containing lipopeptides, Pam2Cys12, Pam2CSK, Pam2CSK4, and two forms of MALP-2 (s and f) were synthesized with reference to a previous report (Table 1) [13,17]. Pam2CSK was used as a negative control [17], which has virtually no cytokine-inducing activity (Fig. 1). By ELAM reporter assay, we assessed NF-κB activation potential of these lipopeptides (10–500 nM), and confirmed that all except Pam2CSK possess similar luciferin-activating potentials (data not shown).

IL-6 and IL-12p40 levels were determined by ELISA with the supernatant of the media where BMDC and each of the lipopeptides were co-cultured for 24 h. These cytokines were detected with high levels in the wells with Pam2Cys12, Pam2CSK4, MALP-2s and MALP-2f but not in Pam2CSK (Fig. 1A,B). These lipopeptides neither induced the mRNA of type I interferon (IFN), IL-15 and IL-8 (data not shown) or produced less than the detection limit (<5 pg/ml) of IL-12p70 protein (Fig. 1C).

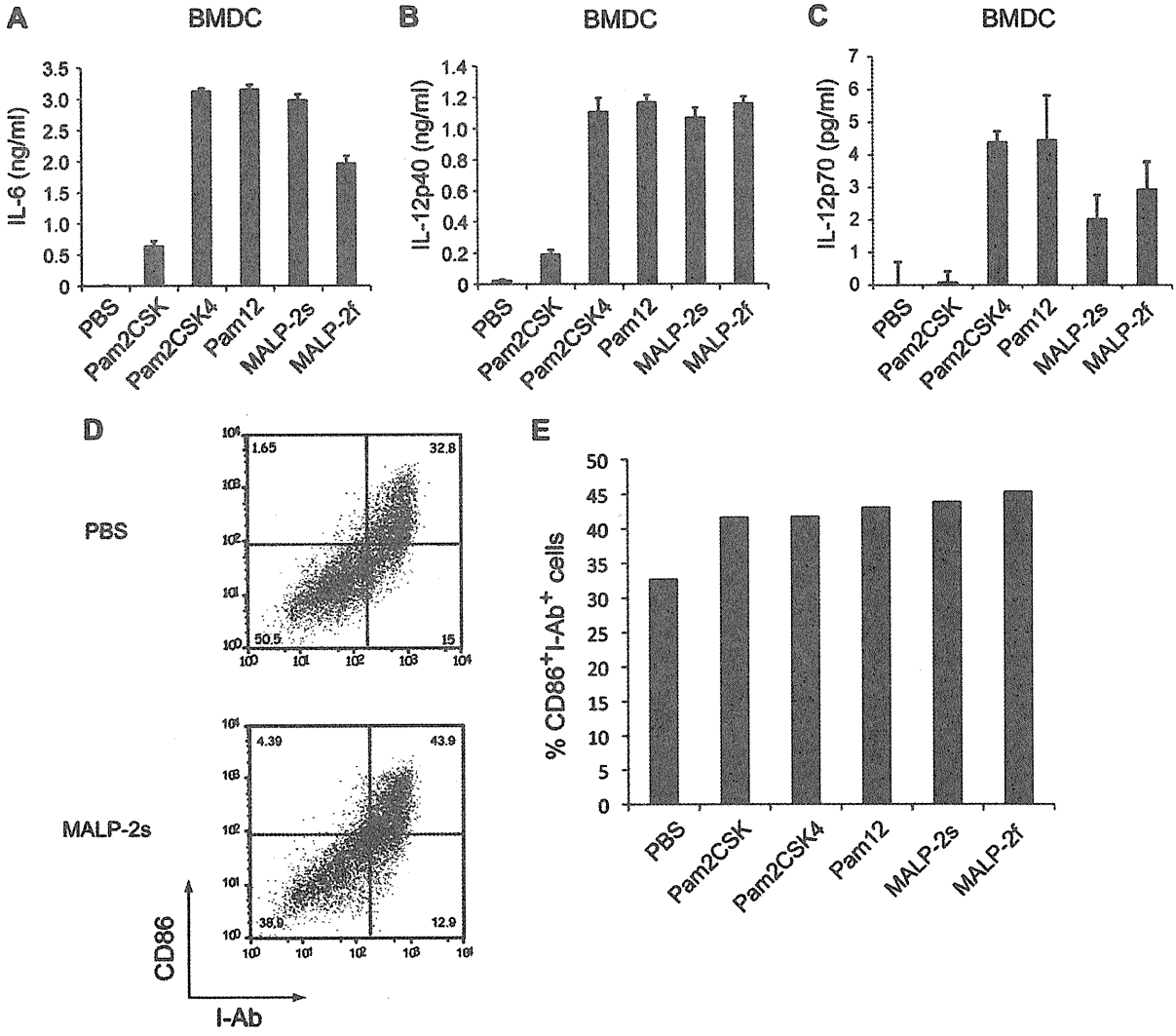

Fig. 1. BMDC cytokine production and maturation in response to TLR2 agonists (A, B, C) Cytokine production by BMDC stimulated with Pam2Cys-containing peptides. BMDC prepared from wild-type mice were treated with indicated Pam2Cys-containing peptides (100 nM) for 24 h. IL-6 (A), IL-12p40 (B), and IL-12p70 (C) concentrations in the supernatant were measured by ELISA. (D, E) Flow cytometric analysis of CD86 and I-Ab expression of BMDC stimulated with Pam2Cys-containing peptides. Typical examples of flow cytometric analysis (D). Summary of CD86 and I-Ab expression on the BMDC (E).

Please cite this article in press as: R. Sawahata, et al., Failure of mycoplasma lipoprotein MALP-2 to induce NK cell activation through dendritic cell TLR2, Microbes and Infection (2011), doi:10.1016/j.micinf.2010.12.003

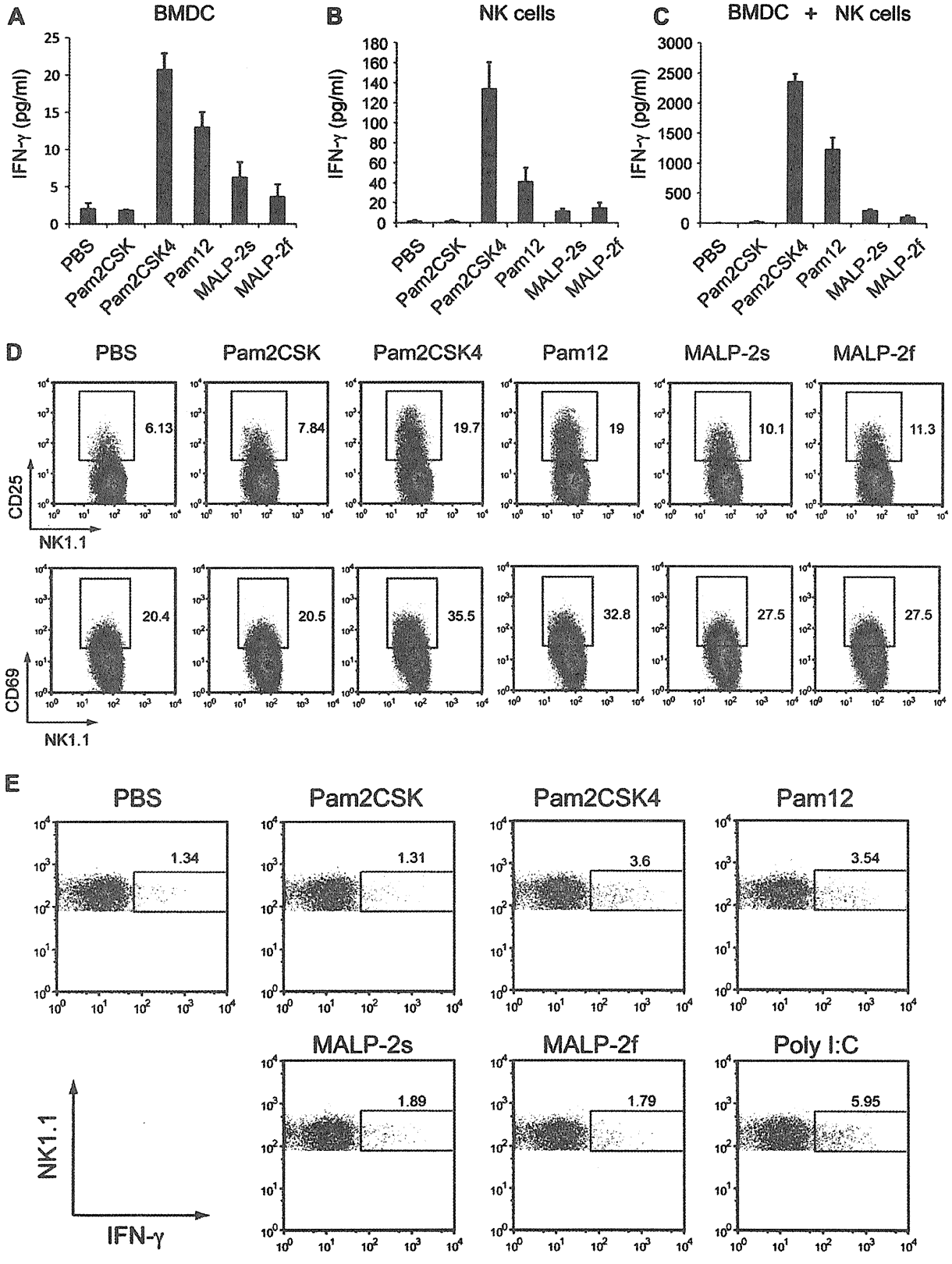

Please cite this article in press as: R. Sawahata, et al., Failure of mycoplasma lipoprotein MALP-2 to induce NK cell activation through dendritic cell TLR2, Microbes and Infection (2011), doi:10.1016/j.micinf.2010.12.003

The degrees of CD86 up-regulation were examined with these lipopeptides, and similar DC maturation was evaluated by flow cytometry (Fig. 1D,E). Although the levels of CD86 were increased in response to Pam2 peptides (100 nM), no significant difference was observed among the Pam2 peptides tested (Fig. 1E). At the dose of Pam2 where cytokine induction sufficiently occurs, CD86 expression inadequately takes place in BMDC, as reported previously [12]. Thus, NF-κB activation, cytokine liberation and DC maturation are partially co-related in these lipopeptides.

3.2. NK activation by Pam2CSK4 and MALP-2

Previous reports suggested that TLR2 agonists have ability to induce NK activation [11,12]. To investigate whether the *Mycoplasma* lipopeptides harbor activity of NK cell activation, we added the Pam2Cys peptides (100 nM) to BMDC, NK cells or BMDC/NK co-culture as in a previous method assessing polyI:C activity for BMDC-mediated NK activation [10]. Although BMDC *per se* can induce IFN-γ production in response to some TLR stimuli [17,18], we could detect only minute amounts of IFN-γ in our setting using Pam2 lipopeptides (Fig. 2A). In this context, three markers for NK activation [19] were assessed with this system, IFN-γ production, up-regulation of NK activation markers and target cell (B16D8) cytotoxicity by NK cells (Fig. 2). IFN-γ was generated in the supernatants (sup) of NK cells (Fig. 2B) or BMDC/NK co-culture (Figs. 2C and 3A left hand panel) in response to the control lipopeptides, Pam2CSK4 and Pam2Cys12. However, MALP-2s and f showed significantly low potentials for IFN-γ-induction comparable to the negative control Pam2CSK.

The NK cell activation markers CD25 and CD69 were analyzed with BMDC co-cultured NK cells with or without the lipopeptide treatment by flow cytometry (Fig. 2D). Up-regulation of surface CD25 and CD69 was observed in NK cells incubated with BMDC stimulated with Pam2CSK4 and Pam2Cys12 but far less with MALP-2s and f.

Activated NK cells are a major source of IFN-γ which causes a variety of responses of the immune system. To further examine whether BMDC matured with Pam2CSK4 or MALP-2 drive NK-dependent IFN-γ secretion, we stimulated BMDC with these lipopeptide reagents for 4 h and then mixed with NK cells (ratio 1:2) for 20 h. Breferdin was added to the mixture in order to accumulate IFN-γ in the NK cells for the last 4 h of incubation. As shown in Fig. 2E, the TLR2 ligands Pam2CSK4 and Pam2Cys12 significantly increased the frequency of IFN-γ-secreting NK cells, while MALP-2f and s showed far less activity to produce IFN-γ in the NK cells.

Cytotoxic activity was evaluated using B16D8 cells as a target [10]. BMDC-activated NK cells (see above) were incubated with B16D8 cells at a ratio of 30:1. Again, MALP-2s and f showed less effective killing against the target (Fig. 3B left hand panel). The other lipopeptides had sufficient killing activity compared to the control polyI:C: one of two examples assayed with different BMDC lots are shown in the figure.

3.3. Participation of TLR2/MyD88 in MALP-2-mediated NK activation

We next examined whether the lipopeptide-mediated IFN-γ secretion was dependent on MyD88 of BMDC. IFN-γ secretion was almost completely abrogated in the co-culture with MyD88−/− BMDC and wild-type NK cells in the presence of Pam2Cys12 and Pam2CSK4 (Fig. 3A), Similar tendencies were observed with MALP-2 peptides, which essentially evoked a minimal IFN-γ production, and the IFN-γ-induction was largely abrogated with MyD88−/− BMDC (Fig. 3A). The results were less prominently reproduced with TLR2−/− BMDC and wild-type NK cells (data not shown). Further confirmation was performed using the mixtures with wild-type NK cells and various lipopeptides. No direct activation of NK cells was observed in the absence of BMDC (data not shown).

The results were further confirmed with NK cytotoxic assay using NK cells co-cultured with Pam2Cys lipopeptide-stimulated BMDC (Fig. 3B). When wild-type BMDC was used as an NK cell cytotoxicity inducer, full NK activation was induced by Pam2Cys12 or Pam2CSK4. MALP-2f and s were found to be inefficient NK activators (Fig. 3B). If wild-type BMDC were replaced with MyD88−/− BMDC, BMDC-enhanced NK cytotoxicity was abrogated (Fig. 3B). The MyD88 pathway in BMDC is crucial for BMDC-mediated NK cell activation.

3.4. Combinational recognition of MALP-2s and f by TLR2 and TLR6

TLR2 recognizes diacyl lipopeptide in combination with TLR6 [20] while TLR2 recognizes triacyl lipopeptide together with TLR1 [21]. We found TLR2/6 cooperate to recognize *Staphylococcus aureus* lipopeptides using HEK293 cells with TLR2/6 expression. Data testing MALP-2f for the usage of TLR2/6 are shown in Fig. 4. Single receptors of TLR1, TLR6 and TLR10 barely activate NF-κB by reporter assay and only TLR2 exhibited <60 fold ELAM promoter activation (data not shown). No enhanced activation was observed in combination with TLR2 and TLR1 or TLR2 and TLR10. Similar results on TLR2/6-mediated augmentation of reporter activation were observed with MALP-2s and Pam2CSK4 (data not shown).

Fig. 2. Pam2Cys-containing peptides activate NK cells through TLR2 in BMDC. (A, B, C) BMDC and NK cells prepared from wild-type mice were stimulated with Pam2Cys-containing peptides for 24 h (A, B). Alternatively, BMDC were stimulated with Pam2Cys-containing peptides for 4 h. Then, NK cells prepared from wild-type mouse spleen were co-cultured with the BMDC for 24 h. IFN-γ levels in the culture supernatant are shown. (D) CD25 and CD69 expression on NK cells co-cultured with BMDC in the presence of Pam2Cys-containing peptides. The NK cell populations (marked with NK1.1) were gated on the display of FACS and levels of CD25 or CD69 (inset values) were examined as shown in the graphs. (E) Intracellular IFN-γ staining of NK cells co-cultured with BMDC in the presence of Pam2Cys-containing peptides as above. Cells were treated with breferdin and then permeabilized. Intracellular IFN-γ was detected by specific mAb. IFN-γ positive cells are marked with square and their frequencies are indicated by inset values.

Please cite this article in press as: R. Sawahata, et al., Failure of mycoplasma lipoprotein MALP-2 to induce NK cell activation through dendritic cell TLR2, Microbes and Infection (2011), doi:10.1016/j.micinf.2010.12.003

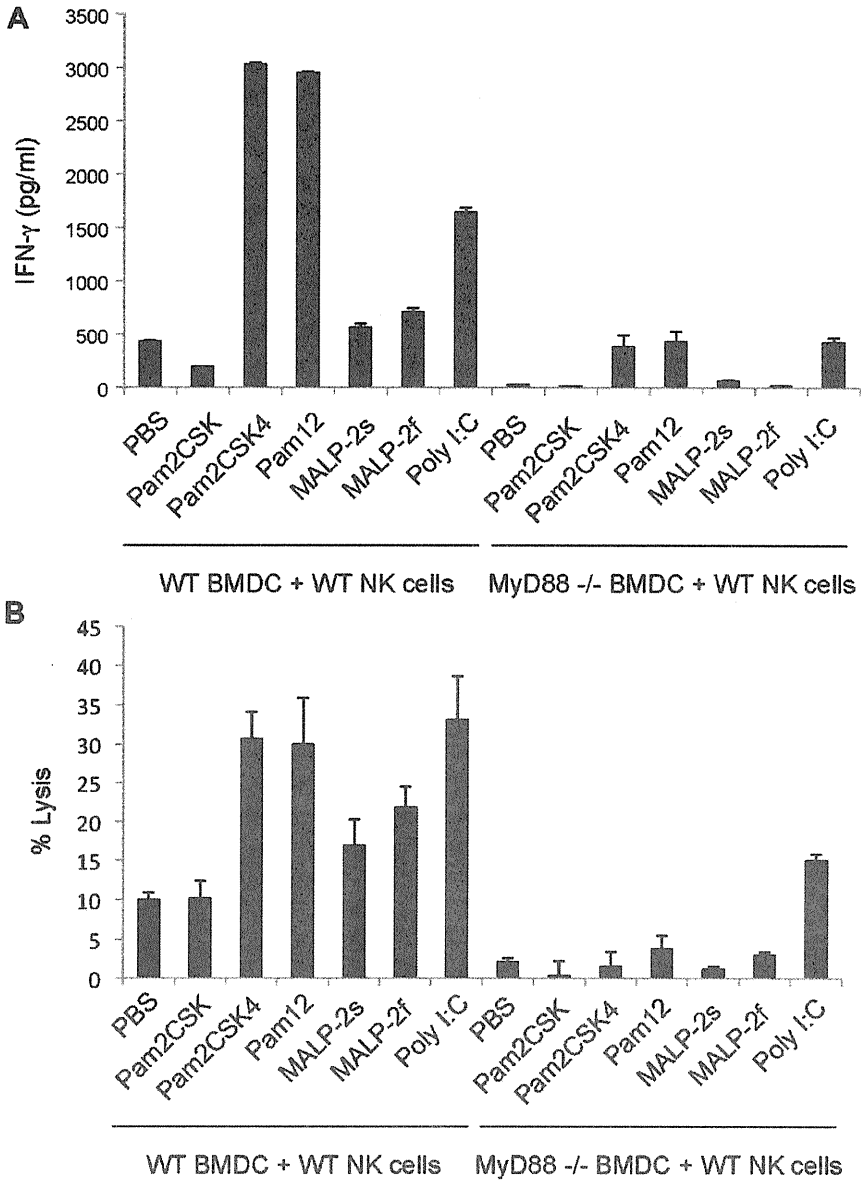

Fig. 3. IFN-γ production and cytotoxic activity of NK cells co-cultured with BMDC in the presence of Pam2Cys-containing peptides. Wild-type and MyD88−/− BMDC were stimulated with Pam2Cys-containing peptides for 4 h. Then, the BMDC were co-cultured with wild-type NK cells for 24 h (A) IFN-γ levels in culture supernatant were determined by ELISA. (B) Cytotoxic activities of NK cells were measured by ^{51}Cr release assay. B16D8 cells were used as a target. E/T ratio = 20.

Hence, TLR6 helps to amplify the TLR2 signal by MALP-2 lipopeptide as in other Pam2Cys lipopeptides, but IFN-γ was minimally induced in the NK cells.

3.5. *Antitumor adjuvant activity against NK-sensitive tumor* in vivo

Recent studies revealed that intratumoral or i.p. injection of MALP-2 supresses pancreatic carcinoma in a mouse model [22]. Tumor suppression is also observed with Pam2Cys type lipopeptides in B16D8 (NK-sensitive) implant mice [23]. The antitumor function by MALP-2 is abrogated in MyD88−/− mice, suggesting that TLR2/MyD88 and following cell-mediated immunity play a major part of tumor suppression [23]. We tested whether MALP-2 injected s.c. induces growth retardation of the tumor (NK target B16D8 cells) via NK activation (Fig. 5). Pam2CSK4 s.c. injected around tumor exhibited tumor growth retardation (Fig. 5A). This Pam2CSK4 activity was abrogated by injection of asialoGM-1 Ab (data not shown). In contrast, no tumor growth retardation was observed in this NK-sensitive tumor by s.c. injected MALP-2 (Fig. 5B). The results infer that MALP-2 exerts only minimal

Please cite this article in press as: R. Sawahata, et al., Failure of mycoplasma lipoprotein MALP-2 to induce NK cell activation through dendritic cell TLR2, Microbes and Infection (2011), doi:10.1016/j.micinf.2010.12.003

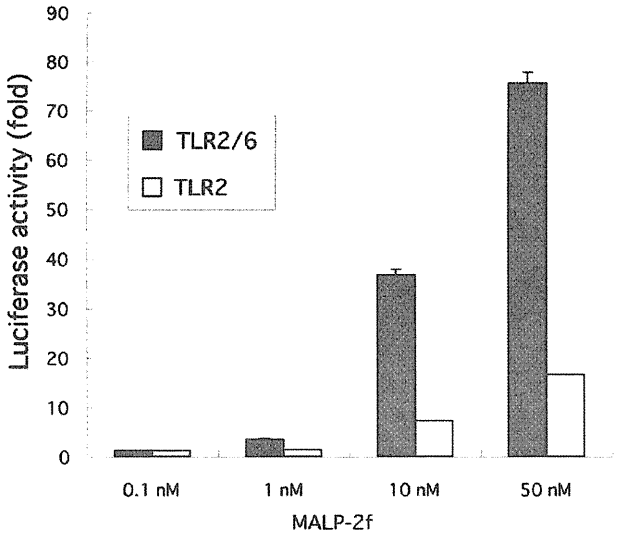

Fig. 4. TLR6 facilitates the recognition of MALP-2 by TLR2. HEK293 cells were transfected with the plasmids encoding TLR2 and/or TLR6, and ELAM-luciferase reporter. After 24 h, the cells were treated with MALP-2f for 6 h. Then, luciferase activity of the cell lysates was measured. Similar results were obtained with MALP-2s (not shown).

potential if any, to activate NK cells through BMDC *in vitro* and *vivo*. Unlike BCG-CWS [19] or polyI:C [8–10], MALP-2 barely suppresses tumor growth in this mouse system.

4. Discussion

Recent studies demonstrated that mDC induce NK activation by stimulation with TLR2 in mDC [12]. This NK activation occurs in a distinct mode of those reported in the TICAM-1/IPS-1 pathways for type I IFN induction because this NK activation is derived through the MyD88 pathway. Indeed, MyD88 has been reported to participate in NK cell activation induced by *Plasmodium falciparum*-infected erythrocytes, but TLR2 response was not mandatory in the reported human case [24]. In another report, direct TLR2 stimulation in NK cells but not mDC was critical for NK cell activation in a vaccinia infection system [25]. We then tested whether a TLR2 agonist MALP-2 harbors adjuvant potential of mDC-mediated NK activation in mouse.

NK activation fails to be induced by MALP-2-stimulated mDC judged by IFN-γ production, up-regulation of NK activation marker CD25 and CD69, and cytotoxicity against the NK target B16D8 cells. Cytokines with NK activation properties such as IFN-α/β, IL-15 and IL-12p70 are not up-regulated in mDC in response to MALP-2, although a regulatory cytokine IL-10 is produced by stimulation with MALP-2 [3,5]. Finally, s.c. administration of MALP-2 did not result in retardation of tumor growth in mice with B16D8 tumor burden. Although Pam2CSK4 having 6 a.a.-stretch following the diacyl residue acts as an NK-activating reagent [10,18], two forms of MALP-2 with short (6 a.a.) or long (14 a.a.) peptide barely exhibits antitumor activity. Hence, NK activation is a phenotype induced by a limited group of Pam2Cys lipopeptides, and the peptide

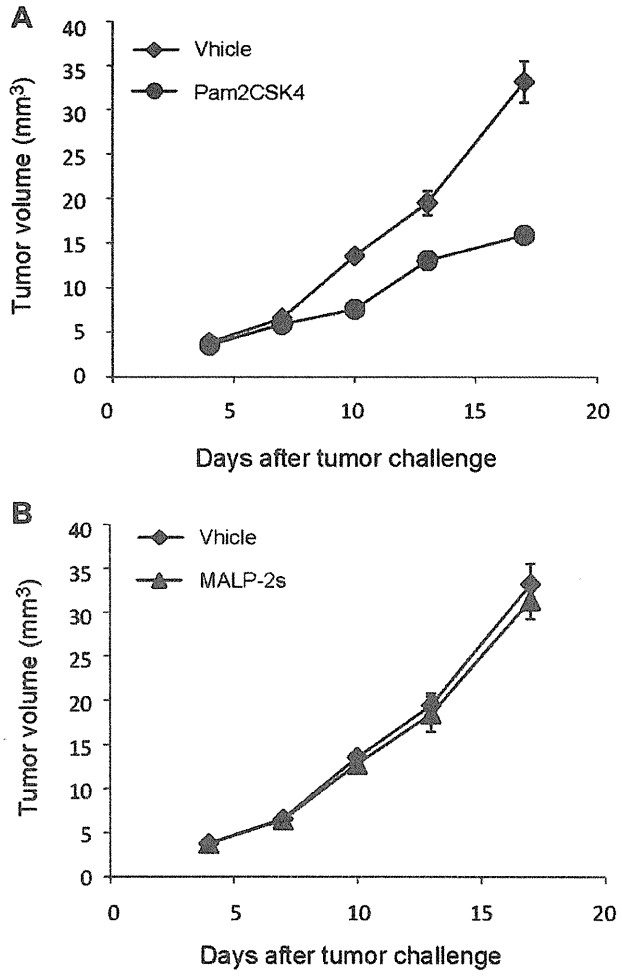

Fig. 5. MALP-2 fails to inhibit tumor growth *in vivo*. B16D8 cells were transplanted subcutaneously into mice at day 0. Mice (16 week-old, female) were treated with Pam2CSK4 (A) or MALP-2s (B) at day 0, 3, 7, 9, 13, 17 as described in Materials and methods. No tumor growth retardation was observed when MALP-2s was replaced with MALP-2f (not shown). Each group consists of $n = 4$. Surface diameters of the implanted tumors were measured. Mean ± SD are shown.

sequence is critical for inducing mDC-mediated NK activation. Our results infer that TLR2-dependent mDC response to drive NK activation largely relies on the peptide sequences of lipoproteins. TLR2-stimulating lipopeptides are not unifunctional: some are active on NK cells but not others.

TLR2 in conjunction with TLR6 serves as an adjuvant receptor with potent cytokine-inducing ability, accompanied with up-regulation of IL-1β, IL-6, IL-12p40 and TNF-α. Apoptosis and NO production are also evoked through TLR2 stimulation [2]. The cytokine profile induced by MALP-2 indicates that macrophages and mDC differentiated from monocytes are targets for MALP-2 via their TLR2. TLR2 agonists facilitate induction of CTL and CD4 T cells against specific antigens [23,26]. In fact, M161Ag potently induces complement-associated inflammation [27] and maturation of immature mDC [16,28]. Although cytoplasmic sensors for bacterial lipoproteins may in part participate in the functional

Please cite this article in press as: R. Sawahata, et al., Failure of mycoplasma lipoprotein MALP-2 to induce NK cell activation through dendritic cell TLR2, Microbes and Infection (2011), doi:10.1016/j.micinf.2010.12.003

properties of MALP-2 [29], TLR2 agonistic activity in MALP-2 would involve cytokine-inducing properties but not anti-tumor function by intensifying *in vivo* NK activation.

Adjuvants are important for induction of vaccine immunity. Cancer immunotherapy has been developed using a variety of adjuvants. Intratumoral or intraperitoneal injection of MALP-2 has been attempted to induce suppression of pancreatic carcinoma in a mouse model [22]. In clinical trials, MALP-2 alone or in combination with gemcitabine was used for the treatment of unresectable pancreas carcinoma [6]. The rationale of this approach is based on the ability of MALP-2 to (1) act as a cytokine inducer [30], (2) activate murine as well as human DC to express co-stimulatory molecules [31], (3) induce a T-helper (Th) 1/2 response [32] and, most importantly, prolong survival in a mouse model of an orthotopic, syngeneic pancreas tumor [22]. Although Pam2 lipoproteins often induce an inhibitory cytokine IL-10 and regulatory T cells (Yamazaki S, unpublished data), no report mentioned the effect of these factors on MALP-2 adjuvant potential. We favored interpretation that the beneficial effects were due to immune activation, as we observed an increase in the expression of co-stimulatory molecules on lymphocytes, and cytotoxic T and NK cells infiltrating the tumor. However, our experiments with tumor-loaded mice showed that s.c. administration of MALP-2 confers no NK cell-mediated tumor regression on B16D8-implant mice. This unexpected result may be due to specific TLR2 agonistic properties of MALP-2 compared to peptidoglycan (that induces IL-12p70 in human mDC) [33] or instability of the lipid moiety of MALP-2. MALP-2 is degraded by two different mechanism in inflamed tissue: de-esterification and oxidation of the thio-ester bridge [6,34], thereby disappearing from the skin with a half time of ~20 h. Further modification will be required for *in vivo* use of this reagent.

Acknowledgments

We thank Drs. J. Kasamatsu, H. Takaki, A. H. Hussein, A. Watanabe and H. Oshiumi in our laboratory for their critical discussions. This work was supported in part by Grants-in-Aid from the Ministry of Education, Science, and Culture (Specified Project for Advanced Research) and the Ministry of Health, Labor, and Welfare of Japan, and by the Yakult and Waxmann Foundations. Financial supports by the Sapporo Biocluster "Bio-S" the Knowledge Cluster Initiative of the MEXT, is gratefully acknowledged.

References

[1] T. Seya, M. Matsumoto, A lipoprotein family from *Mycoplasma fermentans* confers host immune activation through Toll-like receptor 2, Int. J. Biochem. Cell Biol. 34 (2002) 901–906.

[2] M. Matsumoto, M. Nishiguchi, S. Kikkawa, H. Nishimura, S. Nagasawa, T. Seya, Structural and functional properties of complement-activating protein M161Ag, a *Mycoplasma fermentans* gene product that induces cytokine production by human monocytes, J. Biol. Chem. 273 (1998) 12407–12414.

[3] M. Matsumoto, J. Takeda, N. Inoue, T. Hara, M. Hatanaka, K. Takahashi, S. Nagasawa, H. Akedo, T. Seya, A novel protein that participates in non-self discrimination of malignant cells by homologous complement, Nat. Med. 3 (1997) 1266–1270.

[4] K.L. Davis, K.S. Wise, Site-specific proteolysis of the MALP-404 lipoprotein determines the release of a soluble selective lipoprotein-associated motif-containing fragment and alteration of the surface phenotype of *Mycoplasma fermentans*, Infect. Immun. 70 (2002) 1129–1135.

[5] P.F. Mühlradt, M. Kiess, H. Meyer, R. Süssmuth, G. Jung, Isolation, structure elucidation, and synthesis of a macrophage stimulatory lipopeptide from *Mycoplasma fermentans* acting at picomolar concentration, J. Exp. Med. 185 (1997) 1951–1958.

[6] J. Schmidt, T. Welsch, D. Jäger, P.F. Mühlradt, M.W. Büchler, A. Märten, Intratumoral injection of the Toll-like receptor-2/6 agonist 'macrophage-activating lipopeptide-2' in patients with pancreatic carcinoma: a phase I/II trial, Br. J. Cancer 97 (2007) 598–604.

[7] D. Haller, P. Serrant, D. Granato, E.J. Schiffrin, S. Blum, Activation of human NK cells by staphylococci and lactobacilli requires cell contact-dependent costimulation by autologous monocytes, Clin. Diagn. Lab. Immunol. 9 (2002) 649–657.

[8] T. Miyake, Y. Kumagai, H. Kato, Z. Guo, K. Matsushita, T. Satoh, T. Kawagoe, H. Kumar, M.H. Jang, T. Kawai, T. Tani, O. Takeuchi, S. Akira, Poly I: C-induced activation of NK cells by CD8 alpha+ dendritic cells via the IPS-1 and TRIF-dependent pathways, J. Immunol. 183 (2009) 2522–2528.

[9] S. McCartney, W. Vermi, S. Gilfillan, M. Cella, T.L. Murphy, R.D. Schreiber, K.M. Murphy, M. Colonna, Distinct and complementary functions of MDA5 and TLR3 in poly(I:C)-mediated activation of mouse NK cells, J. Exp. Med. 206 (2009) 2967–2976.

[10] T. Akazawa, M. Okuno, Y. Okuda, K. Tsujimura, T. Takahashi, M. Ikawa, M. Okabe, T. Ebihara, M. Shingai, N. Inoue, M. Tanaka-Okamoto, H. Ishizaki, J. Miyoshi, M. Matsumoto, T. Seya, Antitumor NK activation induced by the Toll-like receptor3-TICAM-1 (TRIF) pathway in myeloid dendritic cells, Proc. Natl. Acad. Sci. U S A 104 (2007) 252–257.

[11] Y. Akao, T. Ebihara, H. Masuda, Y. Saeki, K. Hazeki, O. Hazeki, M. Matsumoto, T. Seya, Enhancement of antitumor natural killer cell activation by orally administered Spirulina extract in mice, Cancer Sci. 100 (2009) 1494–1501.

[12] M. Azuma, R. Sawahata, Y. Akao, T. Ebihara, S. Yamazaki, M. Matsumoto, M. Hashimoto, K. Fukase, Y. Fujimoto, T. Seya, The peptide sequence of diacyl lipopeptides determines dendritic cell TLR2-mediated NK activation, PLoS One 5 (2010) e12550.

[13] Y. Fujimoto, M. Hashimoto, M. Furuyashiki, M. Katsumoto, T. Seya, Y. Suda, K. Fukase, Innate immunostimulatory lipopeptides of *Staphylococcus aureus* as TLR2 ligands; Prediction with mRNA expression, chemical synthesis and immunostimulatory activities, Chembiochem 10 (2009) 2311–2315.

[14] O. Takeuchi, K. Hoshino, T. Kawai, H. Sanjo, H. Takada, T. Ogawa, K. Takeda, S. Akira, Differential roles of TLR2 and TLR4 in recognition of gram-negative and gram-positive bacterial cell wall components, Immunity 11 (1999) 443–451.

[15] H. Tanaka, Y. Mori, H. Ishii, H. Akedo, Enhancement of metastatic capacity of fibroblast-tumor cell interaction in mice, Cancer Res. 48 (1988) 1456–1459.

[16] M. Nishiguchi, M. Matsumoto, T. Takao, M. Hoshino, Y. Shimonishi, S. Tsuji, O. Takeuchi, S. Akira, K. Toyoshima, T. Seya, *Mycoplasma fermentans* lipoprotein M161Ag-induced cell activation is mediated by Toll-like receptor 2: role of N-terminal hydrophobic portion in its multiple functions, J. Immunol. 166 (2001) 2610–2616.

[17] D.M. Frucht, T. Fukao, C. Bogdan, H. Schindler, J.J. O'Shea, S. Koyasu, IFN-gamma production by antigen-presenting cells: mechanisms emerge, Trends Immunol. 22 (2001) 556–560.

[18] I. Fricke, D. Mitchell, J. Mittelstädt, N. Lehan, H. Heine, T. Goldmann, A. Böhle, S. Brandau, Mycobacteria induce IFN-gamma production in human dendritic cells via triggering of TLR2, J. Immunol. 176 (2006) 5173–5182.

[19] T. Akazawa, N. Inoue, H. Shime, K. Sugiura, K. Kodama, M. Matsumoto, T. Seya, Adjuvant engineering for cancer immunotherapy: development of

Please cite this article in press as: R. Sawahata, et al., Failure of mycoplasma lipoprotein MALP-2 to induce NK cell activation through dendritic cell TLR2, Microbes and Infection (2011), doi:10.1016/j.micinf.2010.12.003

a synthetic TLR2 ligand with increased cell adhesion, Cancer Sci. 101 (2010) 1596–1603.

[20] O. Takeuchi, T. Kawai, P.F. Mühlradt, M. Morr, J.D. Radolf, A. Zychlinsky, K. Takeda, S. Akira, Discrimination of bacterial lipoproteins by Toll-like receptor 6, Int. Immunol. 13 (2001) 933–940.

[21] O. Takeuchi, S. Sato, T. Horiuchi, K. Hoshino, K. Takeda, Z. Dong, R.L. Modlin, S. Akira, Cutting edge: role of Toll-like receptor 1 in mediating immune response to microbial lipoproteins, J. Immunol. 169 (2002) 10–14.

[22] C. Schneider, T. Schmidt, C. Ziske, K. Tiemann, K. Lee, V. Uhlinsky, P. Behrens, T. Sauerbruch, I. Schmidt-Wolf, P. Mühlradt, J. Schmidt, A. Märten, Tumoursuppression induced by macrophage activating lipopeptide in an ultrasound-guided syngeneic pancreatic carcinoma mouse model, Gut 53 (2003) 355–363.

[23] T. Akazawa, H. Masuda, Y. Saeki, M. Matsumoto, K. Takeda, S. Akira, K. Tsujimura, K. Kuzushima, T. Takahashi, I. Azuma, S. Akira, K. Toyoshima, T. Seya, Adjuvant-mediated tumor regression and tumor-specific cytotoxic response are impaired in MyD88-deficient mice, Cancer Res. 64 (2004) 757–764.

[24] M. Baratin, S. Roetynck, C. Lépolard, C. Falk, S. Sawadogo, S. Uematsu, S. Akira, B. Ryffel, J.G. Tiraby, L. Alexopoulou, C.J. Kirschning, J. Gysin, E. Vivier, S. Ugolini, Natural killer cell and macrophage cooperation in MyD88-dependent innate responses to *Plasmodium falciparum*, Proc. Natl. Acad. Sci. U S A 102 (2005) 14747–14752.

[25] J. Martinez, X. Huang, Y. Yang, Direct TLR2 signaling is critical for NK cell activation and function in response to vaccinia viral infection, PLoS Pathog. 6 (2010) e1000811.

[26] M.H. Wenink, K.C.M. Santegoets, J.C.A. Broen, L. van Bon, S. Abdollahi-Roodsaz, C. Popa, R. Huijbens, T. Remijn, E. Lubberts, P.L.C. M. van Riel, W.B. van den Berg, TR.D.J. Radstake, TLR2 promotes Th2/Th17 responses via TLR4 and TLR7/8 by abrogating the type I IFN amplification loop, J. Immunol. 183 (2009) 6960–6970.

[27] S. Kikkawa, M. Matsumoto, T. Sasaki, M. Nishiguchi, K. Tanaka, K. Toyoshima, T. Seya, Complement activation on *Mycoplasma fermentans* induced mycoplasma clearance from infected cells: Probing the organism with mAbs against M161Ag, Infect. Immun. 68 (2000) 1672–1680.

[28] Y. Nakao, K. Funami, S. Kikkawa, M. Taniguchi, M. Nishiguchi, Y. Fukumori, T. Seya, M. Matsumoto, Surface-expressed TLR6 participates in the recognition of diacylated lipopeptide and peptidoglycan in human cells, J. Immunol. 174 (2005) 1566–1573.

[29] U. Buwitt-Beckmann, H. Heine, K.H. Wiesmüller, G. Jung, R. Brock, S. Akira, A.J. Ulmer, TLR1- and TLR6-independent recognition of bacterial lipopeptides, J. Biol. Chem. 281 (2006) 9049–9057.

[30] F. Rharbaoui, B. Drabner, S. Borsutzky, U. Winckler, M. Morr, B. Ensoli, P.F. Muhlradt, C.A. Guzman, The mycoplasma-derived lipopeptide MALP-2 is a potent mucosal adjuvant, Eur. J. Immunol. 32 (2002) 2857–2865.

[31] H. Weigt, P. Mühlradt, A. Emmendörfer, N. Krug, A. Braun, Synthetic derived mycoplasmal lipopeptide MALP-2 induces maturation and function of dendritic cells, Immunobiology 207 (2003) 1–11.

[32] F. Wittke, R. Hoffmann, J. Buer, I. Dallmann, K. Oevermann, S. Sel, T. Wandert, A. Ganser, J. Atzpodien, Interleukin 10 (IL-10): an immunosuppressive factor and independent predictor in patients with metastatic renal cell carcinoma, Br. J. Cancer 79 (1999) 1182–1184.

[33] S. Tsuji, M. Matsumoto, O. Takeuchi, S. Akira, I. Azuma, A. Hayashi, K. Toyoshima, T. Seya, Maturation of human dendritic cells by cell-wall skeleton of *Mycobacterium bovis* Bacillus Calmette-Guerin: involvement of Toll-like receptors, Infect. Immun. 68 (2000) 6883–6890.

[34] P.F. Mühlradt, M. Kiess, H. Meyer, R. Süssmuth, G. Jung, Structure and specific activity of macrophage-stimulating lipopeptides from *Mycoplasma hyorhinis*, Infect. Immun. 66 (1998) 4804–4810.

Please cite this article in press as: R. Sawahata, et al., Failure of mycoplasma lipoprotein MALP-2 to induce NK cell activation through dendritic cell TLR2, Microbes and Infection (2011), doi:10.1016/j.micinf.2010.12.003

Rev. Med. Virol. 2011; **21**: 67–77.
Published online 10 February 2011 in Wiley Online Library
(wileyonlinelibrary.com)
DOI: 10.1002/rmv.680

Reviews in Medical Virology

REVIEW

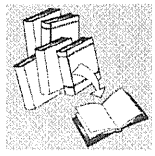

Antiviral responses induced by the TLR3 pathway

Misako Matsumoto*, Hiroyuki Oshiumi and Tsukasa Seya

Department of Microbiology and Immunology, Hokkaido University Graduate School of Medicine, Kita-ku, Sapporo, Japan

SUMMARY

Antiviral responses are successively induced in virus-infected animals, and include primary innate immune responses such as type I interferon (IFN) and cytokine production, secondary natural killer (NK) cell responses, and final cytotoxic T lymphocyte (CTL) responses and antibody production. The endosomal Toll-like receptors (TLRs) and cytoplasmic RIG-I-like receptors (RLRs), which recognize viral nucleic acids, are responsible for virus-induced type I IFN production. RLRs are expressed in most tissues and cells and are primarily implicated in innate immune responses against various viruses through type I IFN production, whereas nucleic acid-sensing TLRs, TLRs 3, 7, 8 and 9, are expressed on the endosomal membrane of dendritic cells (DCs) and play distinct roles in antiviral immunity. TLR3 recognizes viral double-stranded RNA taken up into the endosome and serves to protect the host against viral infection by the induction of a range of responses including type I IFN production and DC-mediated activation of NK cells and CTLs, although the deteriorative role of TLR3 has also been reported in some virus infections. Here, we review the current knowledge on the role of TLR3 during viral infection, and the current understanding of the TLR3-signalling cascade that operates via the adaptor protein TICAM-1 (also called TRIF). Copyright © 2011 John Wiley & Sons, Ltd.

Received: 16 October 2010; Revised: 21 December 2010; Accepted: 21 December 2010

INTRODUCTION

Mammalian cells possess several defense strategies against viral infection, of which, the type I interferon (IFN) system is most important for innate and adaptive antiviral responses [1,2]. Type I IFN induces an antiviral state in uninfected host cells by upregulating IFN-stimulated genes (ISGs) through IFN-α/β receptor signalling, and also activates innate and adaptive immune cells, such as dendritic cells (DCs), natural killer (NK) cells and cytotoxic T lymphocytes (CTLs) [3]. Intrinsic double-stranded RNA (dsRNA) sensors, dsRNA-binding protein kinase R and 2′–5′ oligoadenylate synthetase, are both ISGs, which trigger the shut-down of protein translation and induce RNA degradation within virus-infected cells, respectively [4,5]. Recent progressive studies have demonstrated that the endosomal Toll-like receptors (TLRs) and cytoplasmic retinoic acid inducible gene-I (RIG-I)-like receptors (RLRs) are responsible for virus-induced type I IFN production [6–8]. These receptors recognize viral nucleic acids and induce type I IFN, inflammatory cytokine and chemokine production and DC maturation. TLR3 recognizes virus-derived dsRNA and its synthetic analogue, polyriboinosinic:polyribocytidylic acid (poly (I:C)) [9–11]. dsRNA is found in some virus particles as a viral genome and can be generated

*Corresponding author: M. Matsumoto, Department of Microbiology and Immunology, Hokkaido University Graduate School of Medicine, Kita-ku, Sapporo 060-8638, Japan.
E-mail: matumoto@pop.med.hokudai.ac.jp

Abbreviations:
CT, C-terminal; CTL, cytotoxic T lymphocytes; CVB3, coxsackievirus group B serotype 3; dsRNA, double-stranded RNA; DC, dendritic cell; DUBA, deubiquitinating enzyme A; ECD, ectodomain; EMCV, encephalomyocarditis virus; HCV, hepatitis C virus; HSV-1, herpes simplex virus-1; IAV, influenza A virus; IFN, interferon; INAM, IRF-3-dependent NK-activating molecule; ISG, IFN-stimulated gene; LRR, leucine-rich repeat; MCMV, murine cytomegarovirus; MDA5, melanoma differentiation associated gene 5; NAK, NF-κB activating kinase; NAP1, NAK-associated protein 1; NK, natural killer; NT, N-terminal; NTD, N-terminal domain of TICAM-1; pDC, plasmacytoid DC; poly(I:C), polyriboinosinic:polyribocytidylic acid; PVR, poliovirus receptor; RIG-I, retinoic acid inducible gene-I; RIP1, receptor-interacting protein 1; ss, single-stranded; TBK1, TANK-binding kinase 1; TICAM-1, TIR-containing adaptor molecule-1; TIR, Toll-IL-1 receptor; TLR, Toll-like receptor; RLR, RIG-I-like receptor; WNV, West Nile virus.

during the process of positive-stranded RNA virus and DNA virus replication [12]. TLR7 and TLR8 recognize virus-derived single-stranded (ss) RNA, while TLR9 recognizes non-methylated CpG-containing DNA that is found in some microbes [13–15]. Since these TLRs localize to the endosomal membranes of myeloid or plasmacytoid DCs (pDCs), they appear to detect extracellular viral nucleic acids released from infected cells or virus particles. However, the mechanism by which TLRs encounter virus-derived nucleic acids in endosomes remains to be determined. Interestingly, a recent report showed that TLR7-mediated IFN-α secretion by pDCs in response to ssRNA virus infection requires the transport of cytosolic viral RNA into the lysosome via the process of autophagy [16]. Whether this autophagy-dependent viral recognition is applicable to TLRs 3, 8 and 9 remains unclear.

By contrast, RLRs are expressed in most tissues and cells and detect viral nucleic acids in the cytoplasm. RIG-I recognizes viral RNA genomes bearing 5′-triphosphates and panhandle structures and also short-length dsRNAs [17–21], while melanoma differentiation-associated gene 5 (MDA5) detects long-length dsRNAs and poly(I:C) [22]. Studies using gene-disrupted mice and cells revealed that RIG-I is essential for the detection of various negative-stranded RNA viruses including influenza A virus (IAV), Sendai virus and vesicular stomatitis virus and a positive-stranded RNA virus, hepatitis C virus (HCV), whereas MDA5 plays a key role in sensing encephalomyocarditis virus, a member of *Picornavilridae* family [23–26]. Thus, multiple innate immune pathways are implicated in dsRNA responses and each pathway plays a distinct role in antiviral responses. In this review, we focus on TLR3, whose antiviral function has been controversial, but recent studies have demonstrated the critical role of the TLR3–TICAM-1 pathway in antiviral responses and the induction of adaptive immunity.

Expression and subcellular localization of TLR3

Human TLR3 mRNA has been detected in various tissues including the placenta, pancreas, lung, liver, heart and brain [27]. Interestingly, in the human central nervous system, TLR3 is expressed constitutively in neurons, astrocytes and microglia, suggesting a role in the response to viruses causing encephalopathy [28–30]. In immune cells, only myeloid DCs and macrophages express TLR3. The pDCs, which express TLR7 and TLR9 and secrete large amounts of IFN-α in response to viral infection, do not express TLR3 [31–35]. TLR3 is also expressed in fibroblasts and a variety of epithelial cells, including airway, corneal, cervical, biliary and intestinal cells [10,36–38], which are target sites of virus infection. TLR3 localizes both on the cell surface and endosomes in fibroblasts, macrophages and some of epithelial cell lines. Cell surface-expressed TLR3 participates in dsRNA recognition, as shown by the finding that an anti-human TLR3 monoclonal antibody (mAb) (TLR3.7) inhibits poly(I:C)-induced IFN-β production by fibroblasts [10]. By contrast, myeloid DCs only express TLR3 intracellularly [35]. Subcellular localization analysis showed that endogenous human TLR3 localizes to the early endosome but not to late endosomes/lysosomes in HeLa cells [39], while transfected human TLR3 predominantly localizes to multivesicular bodies in the mouse B-cell line Ba/F3, in which TLR3 was stably expressed at high levels. In any case, TLR3 signalling arises in the endosomal compartment, requiring endosomal maturation [35]. The 'linker' region consisting of 26 a.a. between the transmembrane domain and the Toll-IL-1 receptor (TIR) domain of TLR3, determines intracellular localization of TLR3 [40,41]. An unidentified molecule associating with the linker region may regulate the endosomal retention of TLR3 in myeloid DCs.

Notably, TLR3 expression is upregulated by viral infection and the exogenous addition of poly(I:C) or type I IFN [42]. The IFN-responsive element is located at approximately −30 bp in the human *TLR3* promoter region [43,44].

Recognition of dsRNA by TLR3

TLR3 recognizes dsRNA through its ectodomain (ECD), which induces receptor dimerization required for adaptor-mediated signal transduction [45]. TLR3 consists of an ECD formed by 23 leucine-rich repeats (LRRs) and N- and C-terminal flanking regions, known as the LRR N-terminal (LRR-NT) and C-terminal (LRR-CT) regions, the transmembrane domain and the cytoplasmic TIR domain [46] (Figure 1A). TLR3–ECD possesses 15 putative carbohydrate-binding motifs. Structural analyses

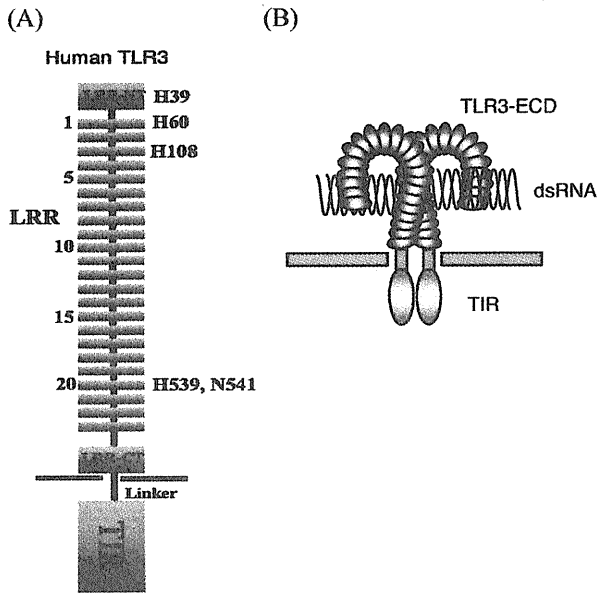

Figure 1. (A) Schematic structure of human TLR3. TLR3 is a type I transmembrane protein of 904 a.a. TLR3 consists of an ECD formed by 23 LRRs and N- and C-terminal flanking regions (LRR-NT and LRR-CT), the transmembrane domain, cytoplasmic linker region and the TIR domain. H539 and N541 in TLR3-LRR20, H39 in the LRR-NT, H60 in LRR1 and H108 in LRR3 are essential for dsRNA-binding. (B) Model of the dsRNA–TLR3-signalling complex. dsRNA interacts with both an N- and a C-terminal binding site on the glycan-free surface of each TLR3–ECD, which are located on opposite sides of the dsRNA (53).

of human TLR3–ECD revealed that the LRRs form a large horseshoe-shaped solenoid of which one face is largely masked by carbohydrate, while the other face is unglycosylated [47,48]. By point mutation analysis, Bell *et al.* [49] demonstrated that the His539 and Asn541 residues in TLR3–LRR20, located on the glycan-free lateral face, are critical amino acids for dsRNA binding and signalling. Wild-type TLR3–ECD protein directly binds poly(I:C) at pH7.6, while mutant proteins H539E and N541A fail to bind poly(I:C). Based on the observation that an acidic pH (pH 6.0 and below) is required for TLR3 recognition of dsRNA, the N-terminal conserved histidine residues, His39 in the LRR-NT, His60 in LRR1 and His108 in LRR3, were identified as a second binding site for dsRNA [50,51]. Protonation of these imidazole groups under acidic conditions, such as those found in endosomes, appears to generate an ionic interaction between the histidine residues and the negatively charged phosphate backbone of dsRNA.

In addition, Leonard *et al.* [52], showed that TLR3–ECD binds as a dimer to 40–50 bp length of dsRNA, and multiple TLR3–ECD dimers bind to long dsRNA strands. Binding affinities increase with both buffer acidity and dsRNA length. At the pH within early endosomes (~6.0–6.5), >90-bp length of dsRNA is required to form a stable complex with TLR3. However, at the pH within late endosomes (~5.5 and below), 40–50-bp length of dsRNA forms stable complex with dimeric TLR3, suggesting that dsRNA-induced TLR3-mediated signalling depends on the length of the dsRNA and the TLR3 localization site [52]. Finally, structural analysis of the complex of two mouse TLR3–ECDs and one 46-bp dsRNA oligonucleotide revealed that dsRNA interacts with both an N- and a C-terminal binding site on the glycan-free surface of each mTLR3–ECD, which are located on opposite sides of the dsRNA [53] (Figure 1B). The dsRNA in the complex retains a typical A-form DNA-like structure. dsRNA has been predicted to adopt a right-handed A-form helix with 11 bp per helical turn and a 28 Å helical pitch [54]. Therefore, two helical turns would fit between the N- and C-terminal binding sites of TLR3 [53]. In addition, the two LRR-CT domains are brought into proximity and form a series of protein–protein interactions, which facilitate the dimerization of the cytoplasmic TIR domain. Funami *et al.* [40], reported that the Phe732, Leu742 and Gly743 residues in the TLR3 cytoplasmic linker region are essential for TLR3 signalling, suggesting that the linker region controls the dimerization of the TLR3–TIR domain.

TLR3–TICAM-1-signalling pathway

TLR3 mediates signalling via an adaptor protein, TIR-containing adaptor molecule-1 (TICAM-1; also called TRIF) [55,56] (Figure 2A). TICAM-1 activates the transcription factors IRF-3, NF-κB and AP-1, leading to the induction of type I IFN, cytokine/chemokine production and DC maturation, which then enables the activation of NK cells and CTLs. TLR3 also associates with c-Src tyrosine kinase on endosomes in response to dsRNA [57]. The Src kinase inhibitor markedly inhibits dsRNA-elicited phosphorylation of Akt, a downstream target of phosphatidylinositol 3-kinase (PI3-K). In addition, PI3-K is required for full phosphorylation and activation of IRF-3 by dsRNA [58]. The precise role of c-Src in IRF-3 activation via the PI3-K-Akt pathway requires further elucidation.

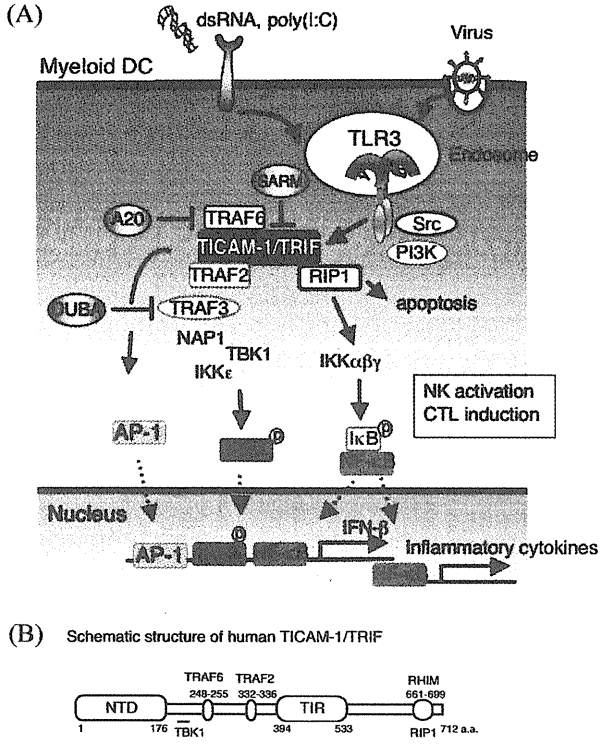

Figure 2. (A) TLR3–TICAM-1-signalling pathway. In myeloid DCs, TLR3 is expressed in the endosomal compartments and recognizes extracellular viral dsRNA and its synthetic analogue poly(I:C). Once TLR3 is dimerized by dsRNA, it recruits the adaptor protein TICAM-1/TRIF that activates the transcription factors, IRF3, NF-κB and AP-1. RIP1 associates with TICAM-1 via the PHIM domain in the C-terminal region and acts as an NF-κB activator and apoptosis mediator in TICAM-1-mediated signalling. TRAF3 and NAP1 participate in the recruitment and activation of the IRF-3 kinases TBK1 and IKKε. Phosphorylated IRF-3 translocates into the nucleus and together with NF-κB and AP-1 induces IFN-β gene transcription. The TICAM-1-mediated AP-1 activation pathway is unclear. (B) Schematic structure of human TICAM-1/TRIF. N-terminal domain (NTD) (1–176 a.a.), TIR domain (394–533 a.a.), RHIM domain (661–699 a.a.), TRAF6-binding site (248–256 a.a.), TRAF2-binding site (332–336 a.a.) and TBK1-binding site (under line) are shown.

TICAM-1 consists of an N-terminal region, a TIR domain and a C-terminal region (Figure 2B). The TIR domain of TICAM-1 is essential for binding to the TIR domain of TLR3 and also to the TLR4 adaptor TICAM-2 (also called TRIF-related adaptor molecule) [59,60]. TICAM-1 is expressed at a low level in most tissues and cells and is diffusely localized in the cytoplasm of resting cells [39]. When endosomal TLR3 is activated by dsRNA, TICAM-1 transiently co-localizes with TLR3, then dissociates from the receptor and forms speckled structures that co-localize with downstream-signalling molecules [39]. Homo-oligomerization through the Pro434 residue in the TIR domain and the C-terminal region is essential for TICAM-1-mediated activation of NF-κB and IRF-3 [61]. Once TICAM-1 is oligomerized, the serine-threonine kinases, TANK-binding kinase 1 (TBK1; also called NAK or T2K) and IkB kinase-related kinase-ε (IKK-ε; also called IKK-i), are activated and phosphorylate IRF-3 [62,63]. The ubiquitin ligase of the TRAF family members, TRAF2, TRAF3 and TRAF6, are downstream-signalling molecules of TICAM-1. TRAF2 and TRAF6 directly bind to the N-terminal region of TICAM-1 [64,65] (Figure 2B). The Lys63-linked autoubiquitination of TRAF3 is required for IRF-3 activation [66,67]. Furthermore, NF-κB-activating kinase (NAK)-associated protein 1 (NAP1) participates in the recruitment of IRF-3 kinases to the N-terminal region of TICAM-1 [68]. Although both TRAF3 and NAP1 associate with oligomerized TICAM-1 and serve as a critical link between TICAM-1 and downstream IRF-3 kinases, there is no evidence that they bind directly to TICAM-1. Interestingly, recent reports showed that direct binding of TBK1 to TICAM-1 is necessary for IRF-3 activation [69]. The Leu194 residue in the N-terminal region is critical for TBK1 binding to TICAM-1. In addition, the Ser189, Arg195 and Ser196 residues are involved in TBK1–TICAM-1 binding.

The N-terminal 176 a.a. of TICAM-1 form a protease-resistant structural domain, designated NTD (Figure 2B). Because the crucial amino acids for TRAF2-, TRAF6- and TBK1-binding reside between the NTD and the TIR domain, naive TICAM-1 may have a closed conformation that covers these binding sites. Indeed, protein–protein interaction analysis revealed that the NTD interacts with the N-terminus of TICAM-1–TIR [69]. Thus, the NTD folds into the TIR domain structure to maintain the naive conformation of TICAM-1. Upon stimulation of TLR3 or TLR4, TICAM-1 oligomerizes through the TIR domain and the C-terminal region, possibly breaking the intramolecular association and inducing a conformational change that allows TBK1 access to TICAM-1.

Whereas the N-terminal region is crucial for TICAM-1-mediated IRF-3 activation, the C-terminal region of TICAM-1 is involved in NF-κB activation and apoptosis. Receptor-interacting protein 1 (RIP1), a kinase containing a death domain, associates with